T.C.

AKSARAY UNIVERSITY

GRADUATE SCHOOL OF NATURAL AND APPLIED SCIENCES

DEPARTMENT OF ELECTRICAL-ELECTRONIC AND COMPUTER ENGINEERING

A SMART ALGORITHM TO PREDICT THE POST-OPERATIVE PARAMETERS OF INTRA-CORNEAL LENS

MASTER THESIS

HALA ZAID ABDULHAMEED

SUPERVISOR

Asst. Prof. Dr. Özlem AKGÜN

AKSARAY, 2019

T.C.

AKSARAY UNIVERSITY

GRADUATE SCHOOL OF NATURAL AND APPLIED SCIENCES

DEPARTMENT OF ELECTRICAL-ELECTRONIC AND COMPUTER ENGINEERING

A SMART ALGORITHM TO PREDICT THE POST-OPERATIVE PARAMETERS OF INTRA-CORNEAL LENS

MASTER THESIS

HALA ZAID ABDULHAMEED

SUPERVISOR

Asst. Prof. Dr. Özlem AKGÜN

AKSARAY, 2019

Aksaray Universıty, Institute Of Science and Technology Approval **Hala Zaid ABDULHAMEED**, M.Sc. with thesis, student No. 162335801, successfully presented the M.Sc. thesis titled "**A SMART ALGORITHM TO PREDICT THE POST-OPERATIVE PARAMETERS OF INTRA-CORNEAL LENS**", prepared after satisfying all the requirements identified in the concerned bylaws, before the jury whose signatures are affixed below.

Thesis Advisor: Asst. Prof. Dr. Özlem AKGÜN

Aksaray University

I approve that this thesis is a Master Thesis in scope and quality ....

Assoc. Prof. Dr. Yunus UZUN

Aksaray University

I approve that this thesis is a Master Thesis in scope and quality ....

Prof. Dr. Mehmet R. TOLUN

Başkent University

I approve that this thesis is a Master Thesis in scope and quality ....

Date of Defence: 25/04/2019

I agree that this theis which is accepted by the jury, has fulfilled the requirements for being a Master Thesis.

....

Assoc. Prof. Dr. M. Ali HINIS

DECLARATION

I declare that I write this work as a master thesis without any help and a way that would be contrary to academic rules and scientific ethics, morals, and tradition.

I declare that I will endure all moral and legal consequence that will arise if this situation is found to be contrary to my statement, regardless of a certain time period by the Institute.

Hala Zaid ABDULHAMEED

ACKNOWLEDGMENT

Special thanks to my supervisor, Dr. ÖZLEM AKGÜN , as well as I would like to thank Dr. Nebras Hussein, for their help, guidance, and supervision.

I would thank my husband, Samer AL-SALIHI, for his patience and endless support, many thanks go to my family for their unconditional love and support all the way through.

Hala Zaid ABDUL HAMEED

AKSARAY, 2019

CONTENTS

M.Sc. THESIS

A SMART ALGORITHM TO PREDICT THE POST-OPERATIVE PARAMETERS OF INTRA-CORNEAL LENS

Hala Zaid ABDULHAMEED

Aksaray University
Graduate School of Natural and Applied Sciences
Department of Electrical-Electronic and Computer Engineering

Supervısor: Asst. Prof. Dr. Özlem AKGÜN

ABSTRACT

Lens implantation has become easier than before due to the studies that conducted to avoid complications when and after the implantation operation,the most inevitable approach to avoid the risk of ICL implantation and overcome the complications is to accomplish the best possible separation between the back ICL surface and the anterior crystalline lens pole which it is called in the terminology of ophthalmology the vault. Recently, machine learning technique is broadly employed in research especially in medical images due to the ability to analyze the data and also using intelligent methods in order to make a suitable decision which assists physicians in the interpretation the images. in this thesis, the machine learning algorithms have been exploited in order to evaluate the postoperative patient eye status, in particular, through building a system with two split phases, feature extraction, and classification. Edge histogram descriptor (EHD) and color layout descriptor (CLD) used for extract the features from the images, whilst, Naïve Bayes and decision tree classifier used for classification, on the other hand, a Hidden Markov Model has employed for diagnoses the Post-Operative eye patient stats via using 3-States after obtaining and mining the characteristics of the input images using singular decomposition value, finally, the precision of the system has calculated for each model.

Keywords: Machine learning, Feature extraction, Naïve Bayes classifier, Decision Tree classifier, Image retrieval, Hidden Markov Model, ICL.

April, 2019; 84 pages

YÜKSEK LİSANS TEZİ

INTRA-CORNEAL LENS'İN POST-OPERATİF PARAMETRELERİNİ KORUMA İÇİN AKILLI BİR ALGORİTMA

Hala Zaid ABDULHAMEED

Aksaray Üniversitesi
Fen Bilimleri Enstitüsü
Elektrik-Elektronik Ve Bilgisayar Mühendisliği

Danışman: Dr. Öğr. Üyesi Özlem AKGÜN

ÖZET

İmplantasyon operasyonu esnasında ve sonrasında meydana gelebilecek komplikasyonları önlemek amacıyla gerçekleştirilen çalışmalar sayesinde, lens implantasyonu eskiye göre daha kolay yapılmaktadır. Burada ICL implantasyonunda risklerden kaçınmak ve komplikasyonların önüne geçebilmek için en önemli yaklaşım arka ICL yüzeyi ile göz bilim terminolojisinde kubbe adı verilen ön kristal lens arasında mümkün olan en iyi ayrımı elde etmektir. Son zamanlarda, görüntü yorumlama konusunda hekimlere yardımcı olacak uygun bir karar verebilmek için veri analizi yapma ve akıllı yöntemler kullanabilme kabiliyetinden dolayı makine öğrenimi tekniği bilhassa tıbbi görüntüleme olmak üzere bilimsel araştırmalarda sıklıkla kullanılır hale gelmiştir. Bu tez çalışmasında, özellik çıkarma ve sınıflandırma olmak üzere iki farklı evreden oluşan bir sistem inşa edilerek hastanın ameliyat sonrası göz durumunun değerlendirilmesi amacıyla makine öğrenimi algoritmaları kullanılmıştır. Görüntülerden özelliklerin çıkarılması için kenar histogramı belirticisi (EHD) ve renk dağılımı belirticisi (CLD) kullanılmış olup sınıflandırma için Naïve Bayes ve karar şeması sınıflandırması kullanılmıştır. Diğer yandan, ameliyat sonrası göz istatistiklerinin teşhisi için tekil değer ayrışımı kullanılarak girdi görüntülerinin özellikleri elde edildikten sonra Saklı Markov Modeli kullanılmış ve son olarak her bir model için sistemin hassasiyet düzeyi hesaplanmıştır.

Anahtar kelimeler: Makine öğrenimi, özellik çıkarma, Naïve Bayes sınıflandırıcısı, karar şeması sınıflandırıcısı, görüntü çağırma, saklı Markov Modeli, ICL.

Nisan, 2019; 84 sayfa

LIST OF FIGURES

LIST OF TABLES

SYMBOLS AND ABBREVIATIONS

AC	Anterior chamber
ACA	Anterior chamber area
ACD	Anterior chamber depth
AIP	Analog image processing
ANN	Artificial Neural Networks
Art	Angular Radial Transformation
CCD	Charge-coupled device camera
CCS	Curvature scale-space
CCV	Color Coherent Vector
CLD	Color Layout Descriptor
CLD	Color Layout Descriptor
CLR	Crystalline lens rise
CSD	Color structure descriptor
DCT	Discrete cosine transform
DIP	Digital image processing
EHD	Edge Histogram Descriptor
FREAK	Fast Retina Key Point
GLCM	Grey level co-occurrence matrix
GUI	Graphics users interface
HMM	Hidden Markov Model
ICL	Implantable Collamer lens
IP	Image Processing
KNN	K-Nearest Neighbourhood
LOCS III	Lens Opacities Classification System III
ML	Machine Learning
MSER	Maximally Stable External Regions
OCT	Optical Coherence Tomography
ORB	Oriented fast and rotated brief
PCA	Principle component analysis
PCO	Posterior capsule opacification
Sand Q	Sampling and Quantization
SIFT	Scale Invariant Feature Transform
STS	Sulcus-to-sulcus distance
SURF	Speeded-Up Robust Features
SVM	Support vector machine
UBM	Ultrasound Biomicroscopy
WTW	White to white

1. INTRODUCTION

A lots of surgical correction of high myopia has substituted by implantable Collamer lens (ICL) implantation due to the success which has achieved by ICL implantation operations (Lackner et al., 2004; Pineda-Fernández et al., 2004), which is made of Collamer and can be implanted inside the human eye where it is a flexible and hydrophilic material, the Collamer is made up of HEMA Hydrogel, water, and porcine collagen (Chen, X. et al., 2016).

Many research has confirmed that despite the many benefits achieved by the lens to patients by implanting in the eye of the patient, but pointed to the postoperative complications in some cases because of the vault (the distance between the posterior surface of the ICL and the anterior surface of the crystalline lens) Lee, H et al. (2014) as shown in Figure 1.1., therefore the vault assessment is an essential manner in order to make the implantation more safety and successful procedure (Alfonso, J. F., 2009).

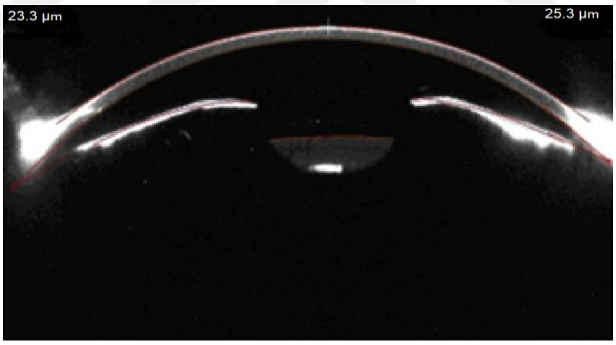

Figure 1.1. The image illustrates the vault.

Depend on vault value the vault categorize into three groups: perfect vault which is describe the value of the vault between 250 µm and 750 µm that the postoperative eyes state be safety (Kojima T and Kugelberg M, 2010; Choi KHet al., 2007; Guell JL et al., 2010) Figure 1.2.a, inadequate vault that its value be <250 µm see Figure 1.2.b which is the most important issue that causes the hazard of cataract development as a result of contact of ICL-crystalline lens or by affecting the lens nutrition development (Gonvers M et al., 2003; Chang J.S. and Meau A.Y., 2007; Sanders D.R., 2008), the third group is excessive vault value as >750 µm that as clarify in Figure 1.2.c possibly will result glaucoma because of impede the lens nutrition caused be blockage nutrition channels, pupillary block, or pigmentary dispersion (Smallman D.S. et al., 2004; Vetter J.M. et al., 2006; Bylsma S.S. et al., 2002; Chung T.Y. et al., 2009).

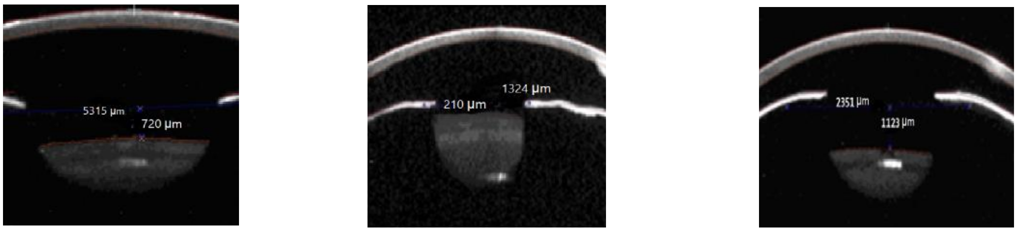

(a) (b) (c)

Figure 1.2. Normal vault valu Inadequate vault value. Excessive value.

There are several ways to assess the vault, in the beginning the vault was measured using traditional technique like slit-lamp which is called subjective method (Zaldivar R et al., 2004; Elies D et al., 2004), then after that the vault had measured objectively by using more recent technique, for instance, optical coherence tomography (Bechmann M, 2002; Koivula A., 2007). Subsequently, the vault is an aspect key to success the ICL implementation, therefore it is required to measure the value of the vault accurately and swiftly through using the capability of the computer and by employing the computer algorithms, methods, and techniques i.e. machine learning techniques or image processing technique.

1.1 Image Processing

Image processing (IP) is a method to perform some operations on an image, in order to get an enhanced image or to extract some useful information from it. Digital image processing means processing the images which are digital in nature by a digital computer. It technique is motivated by two major applications; the first application is improvement of pictorial information for human perception, the second important application Figure 1.3. is for autonomous machine applications (Gonzalez et al., 2008).

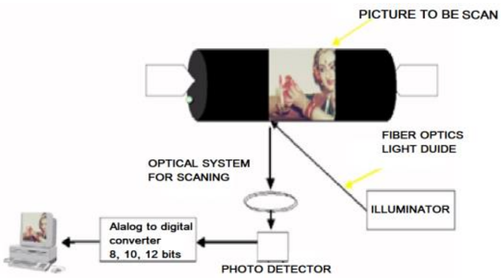

Figure 1.3. Basic image processing technique.

1.1.1 Analog image processing (AIP)

Analog image processing is any image processing task conducted on two-dimensional analog signal by analog means not digital, such as TV images (Rao, 2007).

1.1.2 Digital image processing (DIP)

Digital computers are used to transfer the image into digital one by scanner-digitizer see Figure 1.4. Generally it can be clusterd into few groups: tracking for presence, object detection and localization, measurement, and identification and verification. The preprocess is to enhance the image according to the specific task.The application for identification are barcode and 2-dimenssion matrix code reading, or opticalcharacter recognition.each of these processing techniques coves a wide of machine vision applications, but combining them can give even more possibillities (Rao, 2007). DIP have six main stages, image acquesitin, image enhancement, image restoration, image manipulate, image segmentation, image recognition (Jain et al., 1989, Gonzalez et al., 1992).

1.1.3 Image sampling and quantization (S and Q)

The testing rate decides the spatial goals of the digitized picture, while the quantization level decides the quantity of dark dimensions in the digitized picture. A size of the inspected picture is communicated as a computerized an incentive in picture preparing. The change between consistent estimations of the picture capacity and its computerized equal is called quantization (Kubinger et al. 1998). The notion is replicating the continuous image required to transmission into digital form as seen in Figure 1.4.a.

The quantity of quantization levels ought to be sufficiently high for human view of fine shading subtleties in the picture. The event of false forms is the principle issue in picture which has been quantized with lacking brilliance levels (Kubinger et al. 1998). The function of uni-dimensional in Figure 1.4.b. For sampling, the performance similar intermission may take from the line AB see Figure1.4.c. The resulting digital samples from the processes of the (S and Q) are given in Figure 1.4.d.

An image of two dimensions is yielded by carrying out the method for each line, beginning from the image upper part (Gonzalez et al., 2008).

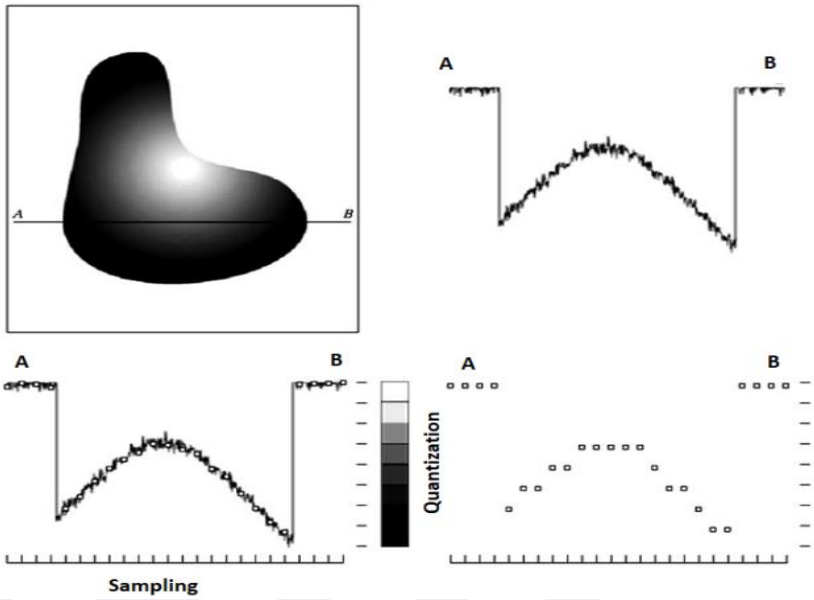

Figure 1.4 Sampling and quantization continuous image to digital scan.

The main capacity performed by the imaging framework is to gather the approaching vitality and center it onto a picture plane. In the event that the brightening is light, the front end of the imaging framework is a focal point, which extends the saw scene onto the focal point central plane. The sensor cluster, which is incidental with the central plane, produces yields corresponding to the necessary of the light got at each sensor. Advanced and simple hardware clear these yields and convert them to a (video) flag, which is then prepared by another segment of the imaging framework. The yield is a computerized picture sees Figure 1.5.a, while in Figure 1.5.b is the sampled and quantized image (Gonzalez et al. 2008). Clearly, the quality of a digital image is determined to a large degree by the number of samples and discrete gray levels used in sampling and quantization.

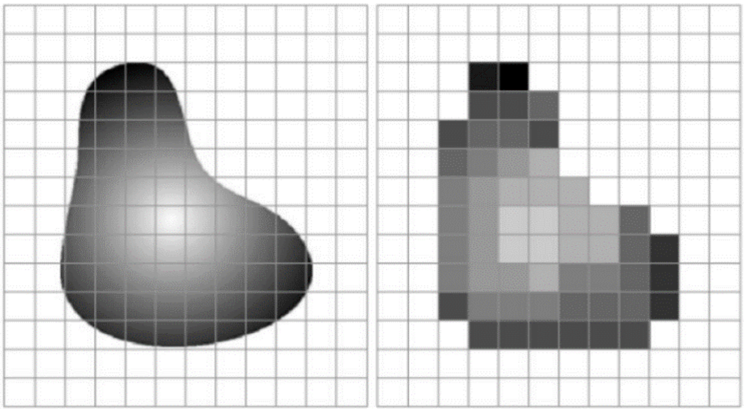

Figure 1.5 Apply sampling and quantization on continues image.

1.2 Machine Learning (ML)

Learning is to learning the knowledge to get the specific objective; the learning has many tasks such as get the information of the internal object, enhancing the system performance etc. AI is an essential field to conquer these def (Lv, H., and Tang, H., 2011; Michalski, R et al., 2013). ML start since the AI field has been started at the 1950s (Martens, H. H., 1959), hat is by using the skills of the computer try to simulate the learning process of the human, which makes the computer to gain important new knowledge, discover fresh knowledge in order to train the system to increase its performance. (Portugal, I. et al., 2017).

ML it becomes one of the important application in AI field (Russell, S. J., and Norvig, 2016), that it an intrusion in many fields straight with computer science for instance business (Apte, C., 2010), advertising (Cui, Q. et al., 2015), and medicine (Kononenko, I., 2001). each method earning information by training the samples which are useful in a learning process in order to estimate the unknown parameters (Duda, R. O. et al., 2012), therefore, learning comes in numerous general forms(Portugal, I. et al., 2017).

1.2.1 Supervised learning

It one of ML tasks, that creates a model to increase the dependencies among training data and the true answer (Kachalsky, I. et al., 2017), through labeling each pattern in a training set (Duda, R. O. et al., 2012).

1.2.2 Unsupervised learning

In unsupervised learning the data are unlabeled, such data its behave similarly to human behavior that can guess the actions by observing a sequence of actions (Parveen, P. and Thuraisingham, B., 2012, June)

1.2.3 Reinforcement learning

In this learning type, the labeled and the goal class label are considered to support the classifier in order to improve it performance (Duda, R. O. et al., 2012), which increases the velocity of the learning process, This property is not available in other types (Jin, Z. J. et al., 2010).

1.3 Machine Learning Algorithms

There are different types of ML in the following we will list some of them.

1.3.1 Naïve Bayes

Naïve Bayes is a classifier that widely used in various fields of science such as robotics control (Liu, B et al. 2014), cloud computing applications, big data and many other fields (Blasch, E. et al., 2013), due to it is the simplest classifier in ML (Liu, B et al. 2013),

For instance total number of classes m where C=$\{c_1, c_2, \ldots., c_m\}$ to the domain D=$\{d_1, d_2, \ldots, d_n\}$, the unique words set is W=$\{w_1, w_2, \ldots., w_s\}$, each of appearing at least one time in the domain D, consequently, the probability of any document d in class c can be obtained by using Bayes' rule:

$$p(c|d) = \frac{p(c)p(d|c)}{p(d)} \qquad (1.1)$$

It is assumed that each word, w_k, in a document occurs independently in the document given the class c. Therefore, the equation becomes:

$$p(c|d) \propto p(c) \prod_{k=1}^{n_d} [p((w_k|c)]^{t_k} \qquad (1.2)$$

Where n_d is the unique words in d, at_k is a frequency of word w_k. To avoid floating point underflow, we use the equivalent equation:

$$\log p\,(c|d) \propto \log p(c) + \sum_{k=1}^{n_d}[t_k \log p\,(w_k|c)] \tag{1.3}$$

So, when applying Na¨ıve Bayes classifier (NBC), we can estimate P(c) and $p(w_k|c)$ as:

$$\hat{p}(c) = \frac{N_c}{N} \quad and \quad \hat{p}(w_k|c) = \frac{N_{wk}}{\sum w_{i\in W} N_{wi}} \tag{1.4}$$

Where N is the total number of documents, N_c is the number of documents

1.3.2 K-means clustering

K-means clustering is an enthusiastically used algorithm in different areas such as medical science, digital image processing, data compression knowledge discovery data mining, and classification. This algorithm is an unsupervised ML algorithm because it allows grouping of objects as they come even it unstructured data and extracts the feature from these data (Bhatia, S., 2014). It was known as Lloyd's algorithm (Lloyd, S., 1982). There are several types of clustering (Xie, J., and Jiang, S., 2010) like Bradley and Fayyad (Bradley, P. S., and Fayyad, U. M., 1998), the GKM algorithm) (Likas, A. et al., 2003), Redmond and Heneghan (Redmond, S. J., and Heneghan, C., 2007), the MGKM algorithm) (Bagirov, A. M., 2008).

1.3.3 Support vector machine (SVM) algorithm

This classifier is uses in many applications (i.e. facial recognition, text recognition,and cancer diagnosis) because it has the power to classify data, this classifire start with preprocessing the data, b efore classifying them into different classes in order to represent these data in Figure 1.6 in a high dimension (Duda, R. O. et al., 2012). Such an algorithm can use for classification tasks that require more accuracy and efficiency of data.

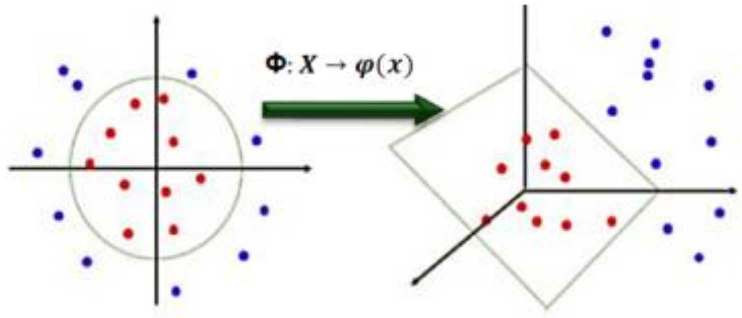

Figure 1.6. Samples with higher dimension space mapping technique in the production process model SVM**.**

This algorithm is suitable for dealing with a small sample of data, which attempt to training the model to overcome the complexity of data (Liu, Z., and Bai, L., 2008).

The SVM designed to solve large margin classification problems as an implementation of statistical learning theory (Boser, B et al., 1992). It establishes a separating hyperplane and a maximal margin free of training data by choosing a subset SV ∈ X called support vectors (Braun, A. Charities et al., 2011).

Equation 1.5 illustrates the optimization problem, and equation 1.6 clarify how to calculate the normal vector with consideration of previous equation.

$$\min \frac{\|w\|^2}{2} + c \sum_{i=1}^{n} \varepsilon_i \qquad (1.5)$$

$$y_i(w.x_i + b) \geq 1 - \varepsilon_i \qquad (1.6)$$

1.3.4 Decision tree algorithm

Decision tree classifier depends on producing a sequence of questions to distinguish the pattern see Figure 1.7 (Duda, R. O. et al., 2012). It is a primary classifier used in ML, that, it decreases the computation by developing a model that enables to control the excessive characteristic (Barros, R. C. et al., 2015).

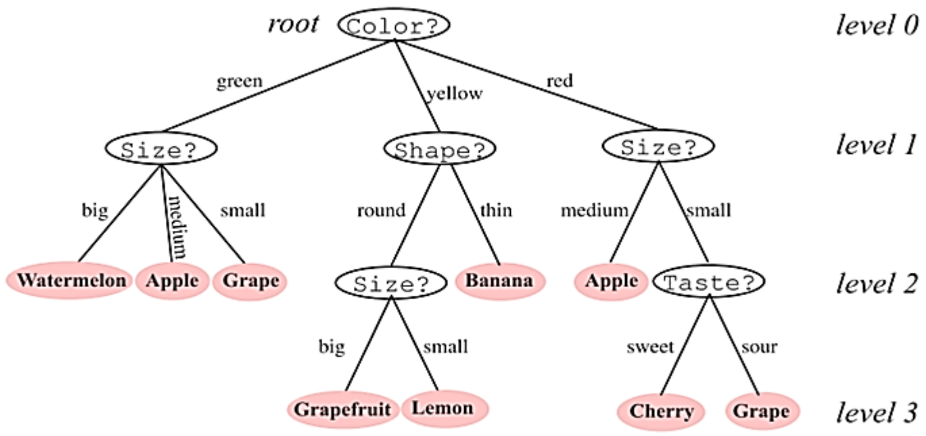

Figure 1.7. Decision tree classification proceeds from top to bottom**.**

In some incidents this algorithm show experience to improve the enforcement of the system to classification method more than the other algorithms (Quinlan, J. R., 1986; Quinlan, J. R., 2014), it is carrying path from root to the leaf that satisfies the decision (Yuan, Y. et al., 2002).

1.3.5 Principle component analysis (PCA) algorithm

PCA is exploit to reduce the high dimensionality of the data, which gives only the variation present in the data set. This achieved by transforming to a new set of variables, the principal components (PCs that this data are unrelated to each other, which order in a way that keeps only a few variations in all the variables. Suppose that x is a vector of p random variables and that the variances of the p random variables and the structure of the covariance or correlations between the p variables are of interest, Figure 1.8 shows the 2-dimensional observation of two variables (Jolliffe, I., 2011).

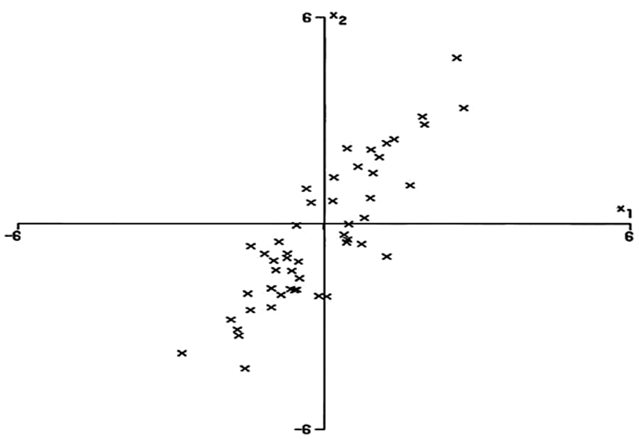

Figure 1.8. Observations on two variables x1, x2.

The first step is to look for a linear function $\alpha_1{}'x$ of the elements of x having maximum variance, where α_1 is a vector of p constants $\alpha_{11}, \alpha_{12}, \ldots, \alpha_{1p}$, and $'$ denotes transpose.

$$\alpha_1{}'x = a_{11}x_1 + a_{12}x_2 + \ldots + a_{1p}x_p = \sum_{j=1}^{p} \alpha_{1j}x_j \qquad (1.7)$$

Reduction complexity achieved by transforming the original variables to PCs Figure 1.9.

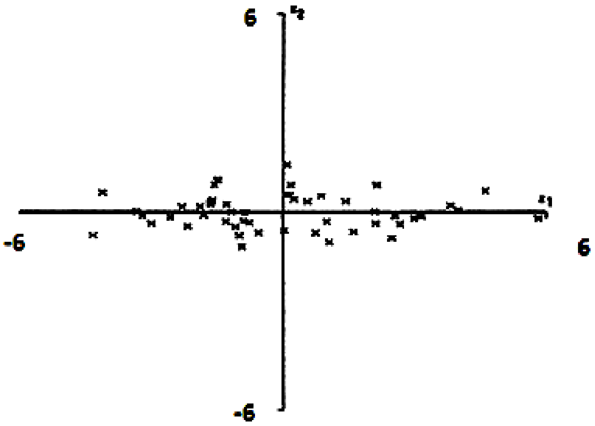

Figure 1.9. Observations with respect to their PCs**.**

1.3.6 Artificial neural networks (ANN)

The structure of the ANN is like any other network, there is an interconnection between nodes which is called neurons and the edge that connect them together. An ANN main function is to receive a set of inputs, perform a progressively complex calculation, and then use the output to solve a problem. ANN is used for a lot of different applications. ANN used for classification tasks where an object can fall into one of at least two different categories, unlike other networks like a social network, an ANN is highly structured and comes in layers see Figure 1.10; the first layer is the input layer, the final layer is the output layer and all layer in between is referred to as hidden layers. An ANN can be viewed as a result of spinning classifiers together in layers web; this is because each node in the hidden and output layer has its own classifier. Any node in hidden layer gets its input from input layer, and activates is score and then pass as input to next hidden layer for farther activations, and this plays out and to end across the entire network to the reach the output layer. The results of the classification are determined by the scores at each node, this happens for each set of inputs, this process is known as forwarding propagation. Forward propagation is a neuron nets way of classifying a set of inputs. In hidden layer each set of inputs is modified by unique weights and biases, that means each edge have a unique weight as well as unique bias, therefore the combination used for each activation is also unique, which explains why the nodes fire differently. The process of improving neuron nets is called training, just like with other machine learning methods. To train the net, the output from forward propagation is compare to the output that is known to be correct and the cost is different for the two, the point of training is to make that cost as small as possible, across millions of training examples, to do this the net tweaks the weight and bias step by step until the prediction closely match the correct output. Once trained well, a neural net has the potential to make accurate predictions each time (Ermini, L. et al., 2005, Kordylewski, H. et al., 2001; Nigam, V. P., and Graupe, D., 2004).

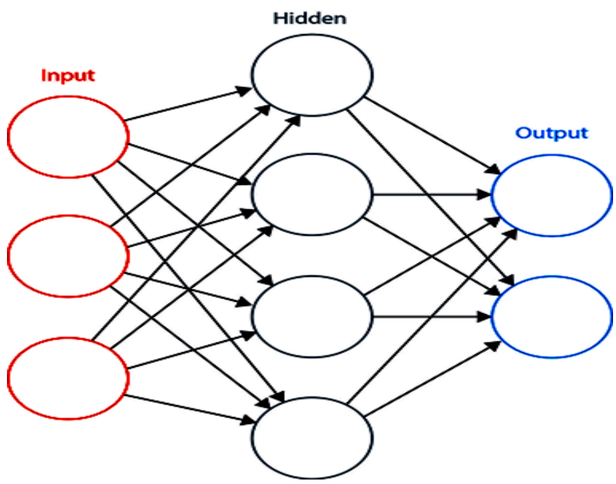

Figure 1.10. An ANN interconnected group of nodes.

1.3.7 K-nearest neighborhood (KNN)

KNN is one of simplest supervised machine learning algorithms, mostly use for classification, it is classifying a data point based on how its neighbor are classified, which store all available cases and classify new bases based on similarity measure, it is perimeter that refers to the number of nearest neighbors to include the majority of the voting process. The KNN algorithm based on feature similarity choosing a right value of k is a process called parameter tuning and it is important for better accuracy, its value is changed depending on where the point drastically changes your answer, k is chosen by using the square root of the total number of values. KNN used when the data labeled (Garcia, V, et al., 2008).

1.3.8 Regression machine learning algorithm

This algorithm attempt to model the relationship between the two variables by setting a linear equation to observed data, one variable considered as an explanatory variable while the other is considered to a dependent variable, the dependent variable is variable that explains the other variables and the values are independent. This algorithm can used in one of two ways; to establish if there is a relation between two variables or see if there is a statistically significant relationship between them, represented by a linear equation.

$$Y = a * X + b. \tag{1.8}$$

Where Y is Dependent Variable, a Slope, X is Independent variable, and b is Intercept. The second way that can use this algorithm is to forecast a new observation (Binary values like 0/1, yes/no, true/false), it predicts the probability of occurrence of an event by fitting data to a logit function, its output values lie between 0 and 1, Logistic regression is used in many applications in machine learning. (Zhang, M. L., and Zhou, Z. H., 2007).

1.3.9 Recommender system algorithm

In this algorithm, the information is filtered and then grouped together and merged to make recommendations to the user. It makes global product-based associations and gives personalized recommendations based on a user's own rating (Sarwar, B, et al., 2001).

1.3.10 Random forest machine learning algorithm

A supervised algorithm uses in many fields it employs the classification and regression to create a forest with a number of trees randomly, the different from decision tree that it finds the roots nodes, it is used in industrial applications such as finding out whether a loan applicant is low-risk or high-risk, predicting the failure of mechanical parts in automobile engines and predicting social media share scores and performance scores (Livingston, F., 2005).

1.4 Image Feature Descriptors

Feature is basically a good place in image that it could reliably find in another image of the same scene taken a different prespective, the whole points defining the features is to be able to make these correspondences between images of the same scene taken from different prespective, the feature of the image that often related to the shape, texture, color, and edge, therefore the descriptor attempt to discover these feature by specific calculations (Kumar, R. M., and Sreekumar, K., 2014).

1.4.1 Color descriptors

The color image can be represent as a set of pixels, color of any pixel in image can lies in range 0 to 255, to extract the feature from color image uses the concept of RGB color wich says that a color can be formed by mixing a spesific percentages of red, green, and blue colors, so each pixel having spesific value of RGB colors, that the feature can extracted using these set of colors.

Using this feature give the descriptor the capability to represent the image (Bober, M., 2001). The Histograms distribute the number of pixels for an image (Ogle, V. E., and Stonebraker, M., 1995), whereas the RGB histogram is a one-dimension histogram has built depend on the frequencies of RGB space. The adversary histogram is a blend of three one measurement histograms of rival shading space. Tint histogram: Associate the shade histogram by its immersion. RGB histogram was invariant to changing the states of light and shading. Changed shading dissemination Reasonable for changing the state of light, on the grounds that each channel is autonomously standardized. In color Coherent Vector (CCV) the histogram is comprise of two classifications the first is reasonable all pixels that have a place with one locale then it is the second class (Pass, G., et al., 1979). In color SIFT Descriptors the introduction histogram is determined to portray the shape; it is not invariant to various light conditions, that the power channel is composite by consolidating the R, G, B channels (Kabbai, L. et al., 2015). In HSV-SIFT there are no invariance qualities of the total descriptor, as a result of the mix of the HSV channels (Guo, X., and Cao, X., 2012). Hue SIFT descriptor is scale-invariant and move invariant, for example, HUV histogram (Van De Sandeet al. 2010). The OpponentSIFT utilizes every one of the channels rival shading space has portrayed by utilizing filter descriptors (El Meslouhi, O., et al., 2010). C-SIFT isn't move invariant, however on the other hand it is scale-invariant as for light (Burghouts, G. J., and Geusebroek, J. M., 2009). Rg SIFT is scale-invariant since the descriptors are added for r and g component, this descriptor is also invariant with respect to light color change condition (Brown, M., and Süsstrunk, S., 2011, June). RGB-SIFT is computed for every RGB channel (Silberman, N., and Fergus, R. 2011).

1.4.2 Texture descriptors

This descriptor can extricate a decent and valuable component for looking, perusing, and recovery the pictures, it likewise can assess the pictures properties, for example, coarseness and smooth (Singha, M., and Hemachandran, K., 2012). There are two sorts, the first is the GLCM (grey level co-occurrence matrix) this descriptor utilized to separate the second request of factual surface estimation, which figures the Rakish second minute, connection, Opposite contrast minute and Entropy (Mohanaiah, P et al., 2012).

The second is Haralick Texture Feature, this descriptor is utilized to remove the example's data from the image by utilizing co-occurrence grid, these element are vitality, relationship, idleness, entropy, backwards contrast minute (Miyamoto, E., and Merryman, T., 2005).

1.4.3 MPEG-7 visual descriptors

The features (e.g. texture, shape, and color) can be gotten by exploiting the MPEG-7, using the content of the image enabling easily to measure the likeness of the images as well as videos. (Bober, M., 2001).

- Visual color descriptors: images that contents color have a very strong aspect to represent it, that it makes easy to retrieve those images based on the color content, which is by rotation, size, and orientation of the image.

- Scalable Color Descriptor (SCD): the haar transform used to generate 255 bins by using HSV color space.

- Dominant Color Descriptor: the distribution of the color through the image is used to browse the image and retrieve it swiftly by describing the local color as well as the global color of the images.
- Color Layout Descriptor (CLD): aim to define the distribution of color in an arbitrarily-shaped.
- CSD (color structure descriptor): used to recitation the regional color features in images.

1.4.4 Visual texture descriptors

It constructs through a variety of the color as well as the set of different intensities (Manjunath, B. S.et al., 2001).

- Texture Browsing Descriptor: A texture may have more than one dominant direction and associated scale. For this reason, the texture image has different direction and scale, therefore, that is why this type of descriptor allows a maximum of two various directions (Wu, P., Manjunath et al., 2000).

- Homogenous Texture Descriptor: used to match the similarity of the image using the more direction value among the different number of direction in the image as well as the regularity, coarseness.

- Edge Histogram Non-Homogenous Texture desceiptor: extracting the edge of the image content which is often influenced by the rotation, this descriptor generate three bins that describe the texture of the image (Sikora, T., 2001).

1.4.5 Visual shape descriptors

Useful information for matching the images based on their shapes (Zhang, S., et al., 2010).

- 3-D Shape Descriptor—Shape Spectrum: generate 100 bins that described the histogram of image shape.

- Region-Based Descriptor: describe the shape based on the image content region.
- Contour-Based Shape Descriptor: described using the MPEG-
- Contour-Based Descriptor: It based on curvature scale-space (CCS) illustrations.

1.4.6 Frequency domain descriptors

Using the bit independently, Euclid distance measurement is not used in frequency domain descriptors. (Boczar, T., 2001).

- Scale Invariant Feature Transform (SIFT): it is an algorithm in computer vision to detect and describe the local feature in the image. David Lowe published the algorithm in 1999; applications include object recognition, robotic mapping, and navigation. For any object on the object can extracted to provided feature descriptor of the object, this description, can be used to identify the object. (Lowe, D. G., 1999).
- SURF Descriptor/Detector (Speeded-Up Robust Features): computation of the SIFT is expensive, therefore sometimes it is unsuitable for some applications. SURF is developed primarily for speed up the SIFT algorithm, by using instead of Difference of Gaussian approach uses a hassian matrix approximation, it uses this to detect interesting points and uses the sum of Haar wavelet that responses for orientation assignment (Dalal, N., and Triggs, B., 2005).
- Maximally Stable External Regions (MSER): it is a simple and very powerful idea that was published by Jerry Mathers and colleagues, which builds on the componentry, uses in many applications to solve a wide baseline stereo, so if we have tow images from very different perspectives (rotated with respect to others). the advantage of having such a wide baseline, is that it allows to well get a better estimate of disparity and hence depth, from the other hand the further apart from sensor are the harder is to establish correspondence between the respective regions in those images. Therefor you have only to search for the pixels from the baselines, it helps to find within two images..

- ORB: oriented fast and rotated brief is very fast binary descriptor based on BRIEF, it builds on the well-known FAST key point detector and the recently-developed BRIEF descriptor (Rublee, E. et al., 2011).
- BRIEF: it is similar to SIFT in performance; it performs an exam between the pixels in the image or smooth image. (Calonder, M et al., 2010).
- FREAK: The Fast Retina Key Point is computed by competently between image intensities ended a sampling pattern (Alahi, A. et al., 2012).

2. LITERATURE REVIEW

ICL is a lens that can be implanted into the human eye, guided by a specialist, because of the Myopia. This lens, therefore, amendment the crystalline lens's function, thus dispensing with the glasses. ICL is located, post-operation, before the crystalline lens and behind the iris; (Lee, H. et al., 2018). Factors whose values are indicators of the success of the operation or not; (Alfonso, J. F. et al., 2012). These factors negatively affect the condition of the patient in the case of when the values are incorrect, for instance the vault, which is one of the most important factors that must be measured immediately after the operation because it indicators the main success rate of the operation; (Lee, H. et al., 2018; Schmidinger, G et al., 2010). In the case of the value of the vault is not within the permissible range (poor vault < 250 µm and unreasonable vault > 750 µm); (Gonvers, M., et al., 2003).It is very dangerous to keep this lens inside the eye and must be treated promptly so as not to cause damage to other parts of the eye, also ensures the absence of complications; (Eissa, S.A et al., 2016). Numerous methods and techniques have been used for measuring, which was categorized into two main methods.

2.1 Objective Method

Modern scanning techniques have used in this method, which is classified based on the type of device that has used:

2.1.1 Optical coherence tomography (OCT)

Researchers in 2009, by using OTC for measuring the vault; Schmidinger et al. (2009), and When the vault is very poor (low value), it causes damage to the crystalline lens. This is due to contact the implanted lens with the front surface of the crystalline lens, which is lead to cataract formation.

After measuring the vault, the values indicate that there is a strong and interconnected relationship between the subjective and objective values; (Alfonso, J. F. et al., 2009).

One year later, when measured at the baseline, no significant difference observed between it and the vault measured during accommodation; (Lindland, A et al., 2010).

After the operations of the patients were followed up cases, the vault measured in both states non-accommodative and in an accommodative state, found that 15.6% of cases that it occurs friction between the implanted and crystalline lenses, It was also observed that the vault did not have a fixed value after surgery but changed over time. For example, a high value of vault goes down and stabilizes after three months; (Kojima, T. et al., 2010).

The same device was employed to measure the value of the vault, and it was discovered that in some circumstances the center vault increased in the case of myopia, because of the motion generated by connecting with the crystalline; (Lindland, A et al., 2012). In the same year, Alfonso and his group followed up patients and measured the vault after a week, a month later, after 3 months, and yearly postoperative, they noticed that there was a significant decrease in the value of vault after the surgery, especially in the first six months. These statuses are seen heavily in the eyes that have a very high vault; (Alfonso, J. et al., 2012). A number of factors have studied, and the effect of a factor on other factors has examined. These factors were WTW (white to white), ACD (anterior chamber depth), and vault, they recorded all the changes in these factors. The important thing in this study is that the vault not affected by other factors, this indicates that there is no correlation between the vault and other factors (Kim, W. K. et al., 2012). While Kwaki and his colleagues, additional to the factors have been studied before them. They studied the effect of the crystalline lens rise (CLR) factor on the vault and found that the CLR directly affects the vault. Therefore, it is recommended to pay attention to this factor when measuring the vault; (Kwak, A. et al., 2012).

Kim et al. employed the OCT in 2013 and studied the of exchange the ICL size to a larger or smaller depending on the value of the vault prior to the operation, they dividing the patients into two groups, the first group smaller ICL exchanged, and the second group larger ICL exchanged. They examined the effect of changing the volume of ICL on the vault and concluded that exchanging the size of ICL to smaller or larger significantly Affects positively on the value of vault after the operation that makes it more ideal value; (Kim, W. K., et al., 2013). The group in the same year studied the benefits of planting ICL in one eye only, and after a day of operation the vault is measured and the size of the ICL is adjusted to be implanted with the other eye. They conclude that this procedure reduces the risk of replacing the ICL for both eyes if it is required to exchange its size, therefore the implantation will be for only one eye not for both; (Kim, W. K. et al., 2013).

The comparison between two types of lenses has done; (V4c ICL and V4 ICL). They studied effectively of each type on the factors such as the ACD and the vault. This comparison was made under different lighting conditions, they ended, that does not mention any difference in the ACD under any of these conditions (photopic and mesopic), on the other hand, the vault of the V4c ICL decreased significantly under the photopic conditions, so they should care about what are the circumstances in which the V4c ICL is implanted; (Lee, H. et al., 2014).

In 2015, a study was carried out to follow the changes that take place in the vault as well as in the ACD during accommodation, where the cases are followed by the eyes in which planted V4c and V4 ICL. It was observed after the tested of 35 eyes implanted V4 ICL and 51 were implanted V4c that the vault is not changed definitely during the accommodation, but clear change gets in the ACD, noting significant reductions in ACD; (Lee, H., et al., 2015). In addition, the vault has evaluated after five years of lens implantation of type (phakic intraocular lens). The results showed that the vault is safe in terms of contact with crystalline if its value was 260 µm; (Lisa, C., et al., 2015).

An experiment was conducted in 2017 to find out what a device (OCT) could give valid results to measure the vault during surgery or not. The tests showed that the OCT is able to provide doctors with true and accurate results, where this device is an auxiliary component of the medical staff can provide them with the appropriate size of the ICL and guide them during the operation; (Tan, T. E. et al., 2017). As well in same period, a study was conducted on V4c ICL, tested the extent of change of both vault and irrigated angle after ICL V4c implantation under different conditions, and concluded from this research that a clear change was observed in both under myopic conditions; (Garcia-De la Rosa, et al., 2017).

A pilot study was conducted in 2018 to determine the effectiveness of the vault on pupil movement during exposure to light. The test performed on 39 eyes. The results showed that the value of the vault changes when the pupil size changes due to exposure to light with uneven intensity. This means that the vault affected when the pupil moves; (Gonzalez-Lopez, F. et al., 2018).

2.1.2 Pentacam

The Pentacam has used to determine the extent of change in the vault after a year of ICL implantation. The value of the vault began to change after one month of surgery. The value of the vault decreased significantly, but after three months, the decrease was very low. Generally, the vault tends to decline after the operation; (Du, G. P. et al., 2012).

In 2015, a group of researchers measured the change that occurs in the value of the vault in both ICL containing hole and ICL that does not contain, which are an implant for patients suffering from moderate to high ametropia. It is concluded that the vault does not change in both lenses. In other words, holes existed or do not exist have effect neither on the vault nor on the refraction; (Kamiya, K. et al., 2015).

In 2016, for measure the vault and anterior chamber (AC) angle width, following V4C ICL implantation, pentacam was employed for this purpose, and the result was the appearance of a relationship between the (AC) angle and the vault; (Eissa, S. A. et al., 2016). As well, a comparison was made on the ICL with the hole and the ICL without the hole, and its effect on changing the value of the vault using a Pentacam device. The value of the vault and the size of the pupil have measured at one day, one week, and one month following the operation. The result has come clear that the value of vault changed when the pupil move. In the end, pupil movement is one of the most important factors that threaten to change the value of vault; (Chen, X., et al., 2016).

2.1.3 Ultrasound biomicroscopy (UBM)

UBM is a technical tool used for imaging of the anterior segment of the eye, it had employed in 2011 to measure the vault and showed that in cases of low pIOL vaulting, a care should take especially with the cases which have vault value under 52 μm, and patient age is over 45 years, that these components increment the hazard for cataract; (Maeng, H. S. et al., 2011).

The prediction of vault value after ICL implantation depends on many biometric factors preoperative, such as (horizontal sulcus-to-sulcus distance (STS) or WTW). The predictability of the vault will not accurate if it based solely on horizontal eye pressure. but the predict should depend on other factors, such as compression by the iris, dampening the effect of the ciliary sulcus structure, or innate ICL vault in order to avoid the incorrect prediction; (Lee, D. H et al., 2012).

The value of the vault had calculated based on the (WTW) factor that recommended by the manufacturer of the ICL, but in a study in 2013, the researchers confirmed, after conducting experiments on 50 eyes suffering from myopia, that the measurement of the vault using the same formula with including sulcus diameter factor gives a higher probability for predicting the vault after operation than predict it based on the white-to-white formula; (Reinstein, D. Z. et al., 2013).

Ghoreishi et al. in 2014 evaluated the size of the ICL (which is important to predict the vault postoperative perfectly) based on WTW once and again relied on STS. The evaluation was performed through a 63-eye test and was divided into three groups based on (WTW group, STS group, and the average of WTW and STS). Based on the results obtained from this experiment, They concluded that the association between WTW and STS is almost non-existent and does not affect the ICL sizing, and ICL sizing based on each (WTW and STS) alone gives unsatisfactory results; (Ghoreishi, et al., 2014).

In 2017 a clinical study was conducted to understand the relationship of the vault with the biometric parameters, (central corneal thickness, (WTW) diameter, keratometer, pupil diameter, sulcus-to-sulcus diameter, anterior chamber depth, anterior chamber area (ACA), and central curvature radius of the anterior surface of the lens (Lenscur) of the eye prior to the operation. During three months the vault was measured using UBM. The researchers found that there is a correlation between the vault after ICL implantation and the biometric parameters during which the value of the vault can be predicted postoperative. The value of the vault can be predicted by using measuring the (ACA, WTW, and Lenscur); (Zheng, Q. Y. et al., 2016).

After all, Lee et al. came after a study in 2018 aimed at dividing clinical factors affecting the vault after surgery. Where the relationship between the vault value postoperative, and a number of factors such as ACD, WTW, and STS have examined. Where 236 eyes patients their vault values were between 250 µm and 750 µm has analyzed using different statistical methods. The results show that when the size of the pupil preoperative is large, greater preoperative ACD, and longer preoperative axial length, the vault will inevitably be high; (Lee, H. et al., 2018).

2.2 Subjective Method

Ophthalmologists are trying to measure vault by using some devices to conduct their researches, where two types of lenses were implanted V3 or V4 for the study of cataract formation, and also for the study of the causes of the formation, where 75 eyes were followed up for three months. The results indicated that the formation of cataract increased during the follow-up period, especially older patients. Therefore, it has recommended making the value of vault higher than 0.15 mm to ensure that there is no friction between the ICL and the crystalline lens; (Gonvers, M. et al., 2003).

In a specific study, the value of the vault was measured over a period of one month, three months, and one year. The focus was also on the change in the vault and its relation to refraction. The result appears that the vault is reduced over time, and the results revealed that the vault does not affect fraction and vice versa; (Kamiya, K. et al., 2009)

Alfonso and his team in their study, which also intended to measure the change in the value of the vault after surgery, revealed that the vault decreased after the third month of lens implantation. It is worth noting that the experiment was conducted on 964 eyes for 36 months; (Alfonso, J. F. et al., 2010).

Finally, research in 2017 examines the relationship between the value of the cellar during the process and its value thereafter. This test has performed on 40 eyes implanted in the lens. Summarize that the two values have a close link and therefore can be used to be as a key aspect for postoperative vault prediction procedure; (Titiyal, J. et al., 2017).

3. MATERIALS AND METHODS

3.1 Materials Techniques

3.1.1 Dataset

The dataset is a collection of cornea image that is used for measuring the vault (Height value between the surface ICL and lens), it has collected from the hospital in Baghdad, which consist of 156 images for different patients captured from different angles by using the Pentacam, there are 69 of those images are content normal vault images, and the rest are content non-normal vault images, it had saved in different folders to be used for training the system in order to get the features of every class and harness it for conducting the matching via classification process.

3.1.2 Pentacam device

One of the tools that are used to get the data for cornea is called Pentacam see Figure 3.1, it is a rotation imaging technology, that can exploit to measure the anterior and posterior corneal surface as well as segment structures, and produce number of images from different angles of corneal, offers a greater opportunity to select image with suitable angle in order to measure ICL vault precisely (Lackner, B. et al., 2005; Barkana, Y.,et al., 2005).

Pentacam obtains the image by rotating charge-coupled device camera (CCD) with synchronous pixel sampling as in Figure 3.1, the system is consist of two cameras, UV-free blue light; the first camera is located in the center, and the second is positioned on rotation wheel, this makes the device capable to get a comprehensive image start from the anterior surface of cornea ended to posterior surface the lens which is the interested area for study (Jain, R., and Grewal, S. P. S., 2009).

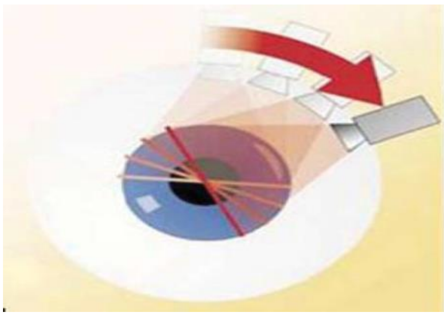

Figure 3.1. Diagrammatic represent rotation camera**.**

The rotation of the camera generates an image with three dimension consist of the number of the slit from zero angles to 360 angle degrees. The software has installed in this device that empowers it to acquire 50 images in two seconds, that generate 138000 true elevation point for interior cornea and the back surface, and its software includes an algorithm that corrects the distortion automatically (Dubbelman, M., and Van der Heijde, G. L., 2001).

Pentacam maintains the center point of a cornea, it not affected by any eye movement during the examination, where the software has technique give the device possibility to reregister the thinnest point and eliminate any eye movement on the contrary of Orbscan.

It is easy for a user to utilize this device as an interface for countless clinical applications. The measurements of factors are an essential part of knowing the eye state and analyzing the cornea of prospective surgery, such as slop (amount of steepness), corneal elevation (a height between two different points), and curvature (changing rate of the slop).

This device can capture 12, 25, 50 images within two second in single scan, therefore many factors can assess using this device, the conditions for using this device is should be followed such as the light condition where the room must be totally dark , patient has asked to locate his chin n the chinrests, and his forehead on the circular ring. The operator should align the instrument in the vertical and horizontal axes, to start calculate the parameters of the posterior corneal surface and anterior surface of the lens.

In order to conduct the ICL implantation operation, there are some preoperative examinations should be calculated such as the anterior chamber angle, which is considered one of the essential factor. The implantation ICL needs precision in terms of location, such this device can clearly determine the location effectively in relation to the crystalline lens and cornea as in Figure 3.2.

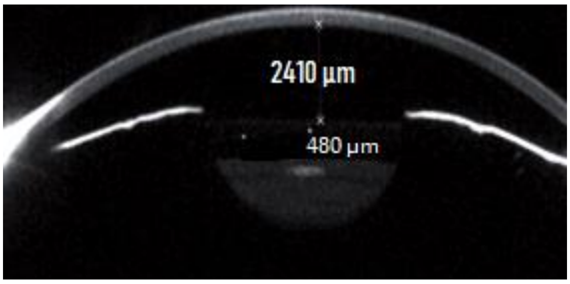

Figure 3.2. ICL and vault value.

In addition, the lens density calculated automatically. A study has shown that the pentacam is butter than LOCS III for predicting the phacoemulsification energy that needs to remove several grades of contract (Grewal, S. P. S.et al., 2006). posterior capsule opacification (PCO) is also can represent, which is much easier than slit-limp images because it is free flash reflection using advance software analysis (Grewal, D. et al., 2008) see Figure 3.3.

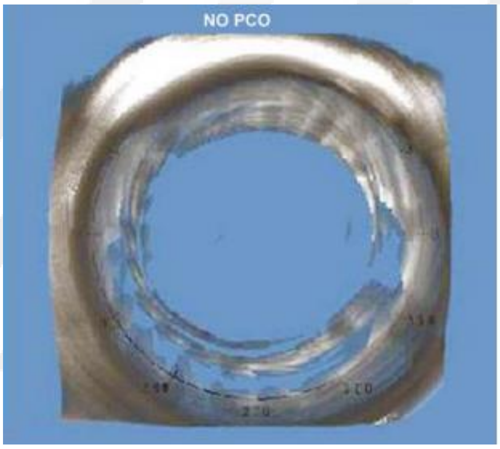

Figure 3.3. Posterior capsule opacification**.**

3.1.3 Feature extraction techniques

Instead of using the value of pixels of the image where it consist of two dimension array, it is more suitable if extract a set of number that is able to represent the characteristics of the image, this set of useful number is called feature vector and the method for extract the characteristic is called feature extraction (Li, X., Chen et al., 2002).

3.1.3.1 Edge histogram descriptor (EHD)

The main function of this descriptor is to illustrate the edges of a present image, where symbols five forms of the edge in each local area, through divided the image into numbers parts each part is ukown as sub-image, the image partitioned into 4x4 non-overlapping chunks see Figure 3.4.

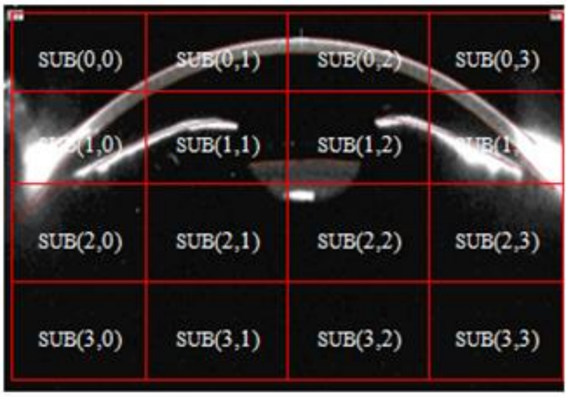

Figure 3.4. An image divided into 16 pieces.

The characteristic is obtained by generating the histogram of the edges for each sub-image, which represent vertical, horizontal, 45-degree diagonal, 135-degree diagonal and non-directional edges as in Figure 3.5.

.

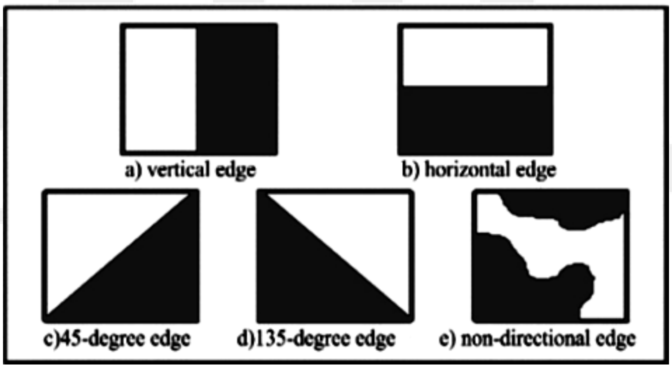

Figure 3.5. Five types of direction.

A histogram has generated from each sub-image see Figure 3.6 that histogram is contained five bines, each bin corresponding one of the five form of the edge.

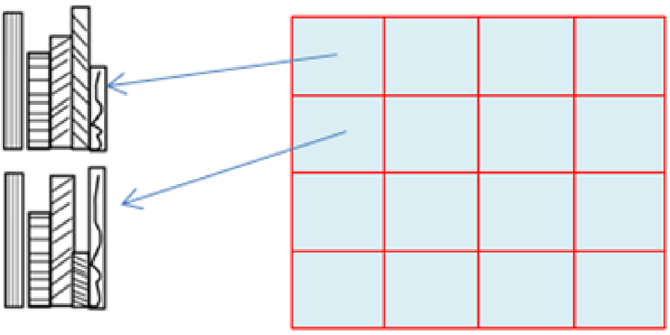

Figure 3.6. Five types of edge bins for each sub-image.

The image is divided into 16 blocks as mentioned above and each block generates five bins concequently, it result a one-dimensional array of 80 bins see Figure 3.7 started from sub-image (0, 0) to (3, 3) sub-image.

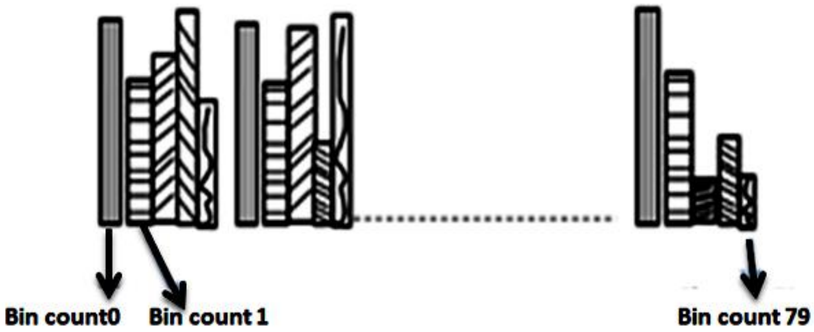

Figure 3.7. The one-dimension array of 80 bins of EHD

These 80 bins are passed in two phases, first one is normalization, it is done by dividing the number of replicates for each type of edge bin over the total number of image–block in sub-image Figure 3.8. The second phase is quantization, due to normalization the values are in small range; therefore, it should be decode bits for each edge type.

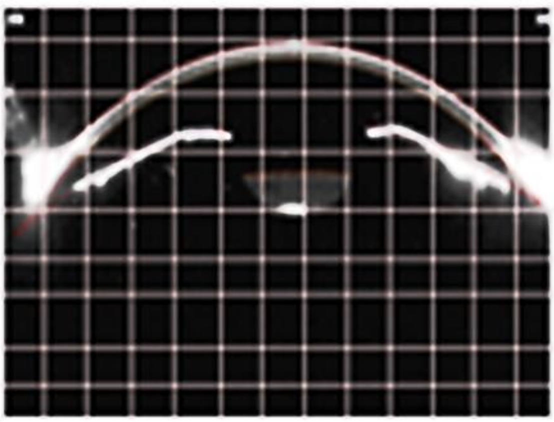

Figure 3.8. Image-block.

3.1.3.2 Color layout descriptor (CLD)

A color image has a very significant aspect that can be used to get a good representation for that image, this factor, is the color, which is clarified the pixels distribution within the image and represent the resolution invariant as well as spatial scattering. The CLD is a suitable descriptor for extracting such characteristics which are utilized in many applications (i.e pattern recognition, computer vision, object detection, and image processing) applications (Kasutani, E., and Yamada, A., 2001).

The procedure for conducting this descriptor is summarized into four phases see Figure 3.9, the first phase is represented by image partitions, that the image divided into 8x8 sub-image, in the second phase is segnified by representive color selection for each individual sub-block, it can use any method to dominate a single color for each block (e.g. pixels average), third stage is construct a three matrices coefficient from handling each sub-block by discrete cosine transform (DCT) after convert it to YCbCr color space, the last and fourth phase is non-linear quantization of the zigzag scanned DCT coefficients (Y, Cb, and Cr), in this phase, the zigzag scanning is used to extract the low frequency from the DCT coefficients, that resulting vector of numbers that consist of 64 numbers that are represent color layout descriptor output as shown in Figure 3.9; (Manjunath, B. Israeli et al., 2001).

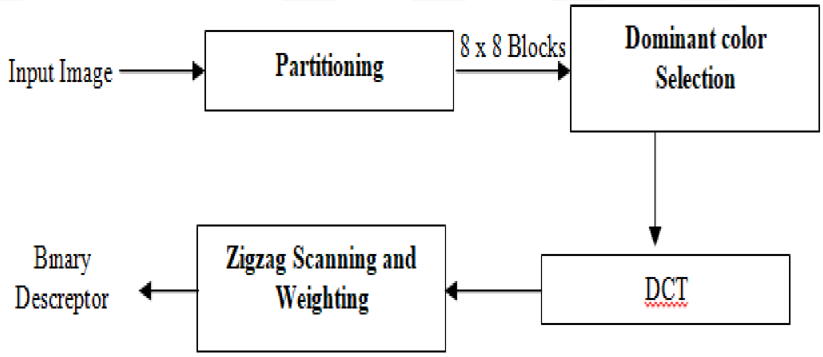

Figure 3.9. Color layout descriptor.

3.1.3.3 Descriptor matching

The matching could be achieved by calculating the distance between two color layout descriptors from different images in order to evaluate whether the two images are similar or not.

$$D = \sqrt{\sum_{K(Y)} W1_i(Y_i - Y_i^t)^2} + \sqrt{\sum_{K(Cb)} W2_i(Cb_i - Cb_i^t)^2} + \sqrt{\sum_{K(Cr)} W3_i(Cr_i - Cr_i^t)^2} \quad (3.1)$$

The matching process is achieved by setting a certain threshold, that's led to identifying whether the images are similar color or not (Manjunath, B. Israeli et al., 2002).

3.1.3.4 Naïve Bayes classifier

Recently, the Naive Bayes classifier becomes very popular due to its simplisity since features are independent given class, Recently, the Naive Bayes classifier becomes very popular due to its simplicity, where the features are processed independently, as well as it achieves a high-quality performance in classifying the data (Friedman, N et al., 1997; Rish, I., 2001).

Due to the independence of the features, the feature trained separately that make this classifier has low computation, especially when it deals with a large amount of data, such a classifier try to make a specific instance belonging to a specific class, that it conducted by calculating the probability of how much this case strongly belonging to a particular class, for a given class, naive Bayes assume that the feature is conditionally independent. Indeed, Naïve Bayes performance is very well repeatedly, that it always presents an excellent accuracy, due to the richness of implementation and it is a small template.

Given an example *X*, described by its feature vector $(X_1, \dots, X_n)$, we are looking for a class *C* that maximizes the likelihood.

$$P(X \mid C) = P(x1, \dots, xn \mid C) \tag{3.2}$$

The Naïve Bayes assumption of conditional independence among the features, given the class, allows us to express this conditional probability $P(X/C)$ as a product of simpler probabilities (Yousef, M. et al., 2006).

$$P(X \mid C) = \prod n_i = 1P(xi \mid C)P(X \mid C) = \prod i = 1nP(x_i \mid C) \tag{3.3}$$

As mentioned before the naive Bayes classifier has proper performance, but there are several factors affect negatively on its performance , these factors summarized into three points; firs is training data noise, which appears when the method of training data be selected in a non-proficient manner, so, it is possible to reduce the training data noise by selecting a suitable method for data training, the other is the bias, this type of errors occurs when the data is crowded because of the magnitude, the lastly is variance, which happens when the data is so small groups. (Mukherjee, S., and Sharma, N., 2012).

The unbalanced (different number of positive and negative example) data is big defiance in training this classifier, that may led to flimsy achievement in its duty (Yousef, M. et al., 2006).

3.1.3.5 Decision tree classifier

Decision tree classifier is one of the machine learning technique; very popular algorithm, which used as multistage search rule (Haralick, R. M., 1976)

According to the DT learning algorithm see Figure 3.10, the root is constructed, then it separates recursively till the end of the algorithm, consequently, a complete decision tree is built (Perner, P., 2014).

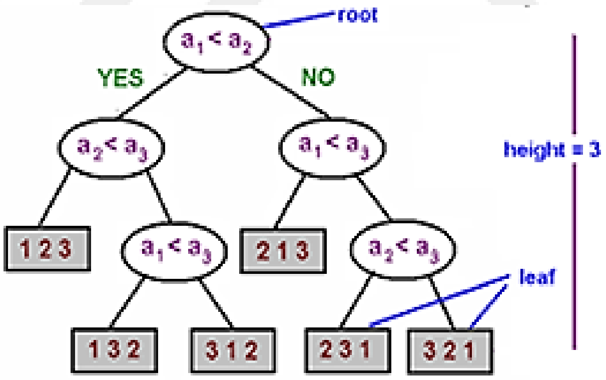

Figure 3.10. Decision Tree.

The objective of the DT classifier is to classify the given dataset correctly, not only can classify the present sample but, beyond could classify the unseen data, easy to the user to make update and have many choices for training the data, finally, try to make the structure simple, therefore the classifier often ready to select appropriate tree structure, and feature subsets should be used at each internal node; (Kurzyński, M. W., 1983).

The DT has many methods for tree structure design such as minimum error rate, min-max path length, the minimum number of nodes in the tree, minimum expected path length, and maximum average mutual information gain etc.; (Quinlan, J. R., and Rivest, R. L., 1989).

The prevalent algorithm of DT is C4.5, which it uses for classification (Li, Y. et al., 2015). This method done by calculating the information of each property for every node in the tree, and then select the most information gain ratio in each node, which is assessed using the rule of entropy; (Safavian, S. R., and Landgrebe, D., 1991). Let us assume that D is a dataset and that Ai is one of the datasets. And there are a set of classes, $C1, C12, \dots \dots, Cm$. The information gain calculated as following.

$$Gain(D, A_I) = Entropy(D) - \sum_{i \in value(A_i)} \frac{|D_i|}{D} Entropy(D_i) \qquad (3.4)$$

Where,

$$Entropy(D) = -\sum_{i=1}^{m} \frac{freq(C_i, D)}{|D|} \log_2 \frac{freq(C_i, D)}{|D|} \qquad (3.5)$$

Where $\mathrm{freq}(\mathrm{Ci}, \mathrm{D})$ denoted the number of examples in the dataset D belongs to class Ci and Di divided by attribute A is value ^{a_i}. Then $\mathrm{SplitInfo}(\mathrm{A_i})$ is defined as the information content of the attribute $\mathrm{A_i}$ itself.

$$SplitInfo(D, A_i) = -\sum_{i \in value(A_i)} \frac{|D_i|}{D} \log_2 \frac{|D_i|}{D} \qquad (3.6)$$

The gain ratio is the information gain calibrated by $\mathrm{splitInfo}$.

$$Gain\ Ratio\ (D, A_i) = \frac{Gain(D,A_i)}{SplitInfo(A_i)} \quad (3.7)$$

3.1.3.6 Hidden Markov model (HMM)

A statistical model that is gives power to the system for observing the series of Hidden (unobservable) states see Figure 3.11. HMM can consider as a simplest dynamic Bayesian network (Krogh, A. et al., 2001).

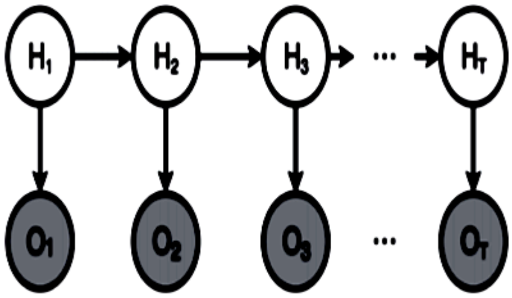

Figure 3.11. Hidden Markov Model.

The system is starting to transfer from state to another state Where in the Figure 3.11. above illustrate the hidden state that is labeled as H_1, H_2, $H_3 \ldots H_r$ and the observed state is labeled as O_1, O_2, $O_3, \ldots . O_r$. Each state has a specific probability over the possible output event. Therefore, HMM generates a series of events that help to give details of the sequence of states, the hidden states indicate to the transition of the model (Tabari, H. et al., 2015). An HMM is generally a Markov chain observed in noise, which is an essential concept in HMM Chain, The next state of the chain depends on the current state, the transition of the model is probabilities which are related to state changing from state to another state (Nguyen, K. A. et al., 2013). An HMM is formally by the following; (Eddy, S. R., 1996).

A hidden state set S $=\{S_1, S_2, \cdot\cdot\cdot, S_N\}$.

A transition matrix A $=\{a_{ij}\}$, which is state transition probability (probability to go from state S_i to state S_j).

$$a_{ij} = P[qt+1 = s_j \,|qt = s_i] \quad 1 \le i,j \le N, \quad a_{ij} \ge 0, \quad \textstyle\sum_{j=1}^{N} a_{ij} = 1 \quad (3.8)$$

An observation events is set of $V = \{v_1, v_2, \cdots, v_M\}$ is called emission matrix, the probability of emission of v_k is $B = \{b_j(k)\}$

$$b_j(k) = P[v_k \text{ at time } t \,|qt = s_j] \qquad 1 \leq j \leq N, \qquad 1 \leq k \leq \qquad (3.9)$$

$$b_i(k) > 0 \text{ and } \sum_{j=1}^{M} b_j(k) = 1 \qquad (3.10)$$

The initial state $\pi = \{\pi_i\}$ is

$$\pi_i = \mathrm{P}[\, q_i = s_i \,] 1 \leq \mathrm{i} \leq \mathrm{N}, \quad \pi_i \geq 0, \quad \sum_{i=1}^{N} \pi_i = 1 \qquad (3.11)$$

HMM is λ = (A, B, π)

The emission with continuous observation is.

$$P(O|j) = b_j(O) = \sum_{m=1}^{M} C_{jm} M[O, \mu_{jm}, \Sigma_{jm}] \qquad (3.12)$$

O is observation vector, $C_{jm}$is the mixture coefficient (Panuccio, A. et al., 2002).

Maximum Likelihood State Assignment (The Viterbi Algorithm) uses for analyzing the sequence of states within the Markov chain that has the very high probability of sequence states, which has the capability to deal with such chain, the sequence of hidden state is known as 'Viterbi path' (Nguyen, K. A., 2013). Viterbi is most common algorithm in HMM; the essence of action of this algorithm is to ask what is the most likelihood of the state z vector that belongs to a specific set. We seek about (Juang, B. H. et al., 1986).

$$argmax_{\vec{z}} P(\overrightarrow{z}|\vec{z}, A, B) = argmax_{\vec{z}} \frac{P(\vec{x}, \vec{z}, A, B)}{\sum_{\vec{z}} P(\vec{x}, \overline{\vec{z}; A, B})} = argmax_{\vec{z}} P(\vec{x}, \vec{z}; A, B) \qquad (3.13)$$

We may try to get the most probable that assigns in the model, so it needs to calculate the set of probabilities.

3.2 Methods

In order to discover a new information about a specific subject or understanding it better, it should be there a particular way to studying by set of specific techniques for selecting cases, measuring and observing aspects, gathering and refining data, and analysing data then reporting on result (Johnson, R. B., and Onwuegbuzie, A. J., 2004), Accordingly, in order to satisfy the objectives of this work, a quantitative research was held, which involves data in the form of numbers and statistics (Taylor, S. et al., 2015), and use precise measurement to predict hypotheses.

3.2.1 Experiment 1: Naïve Bayes and decision tree classifiers

First of all, the dataset partitioning into two separate parts, normal vaults and non-normal vaults, the normal set are images that contain the segment of the cornea with suitable vault, that the vault has value between 250 µ and 750 µ (Kojima T and Kugelberg M, 2010), whereas the non-normal set is images of a segment of the cornea with unsuitable vault. Then a complete system has been built, which is consist of two main phases, the first phase is featuring extraction where the features have extracted from the input dataset for training the system, second phase is classification, where one classifier has been used to conduct the classification process, that predict to which class the test image belong.

There are several algorithms has been built to achieve the aim of the system, firstly, Edge histogram descriptor has employed to extract the characteristics of training dataset, vectors of features was generated, that stored in excel file to be used as an aspect tool for matching and retrieve the content of the test image. After composed the feature vector, the classifier could be used as a tool for classifying the test image see Figure 3.12, in this experiment Naïve Bayes has been used, which is it has the ability to classifying the content of images easily (Lewis, D. D., 1998).

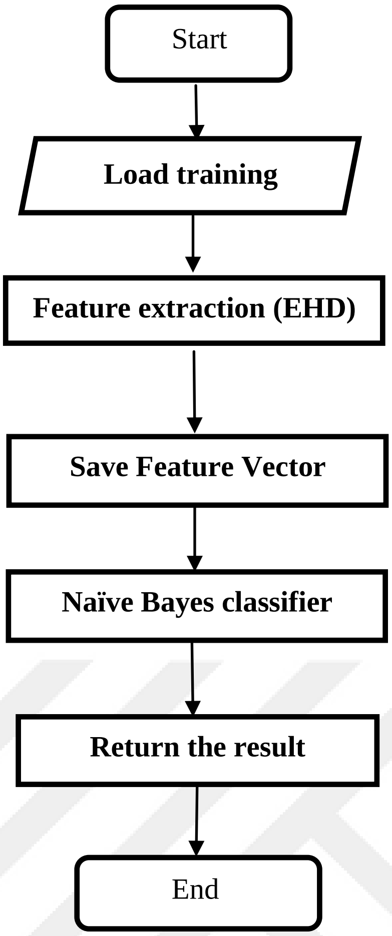

Figure 3.12. Flowchart of EHD with Naïve Bayes classifier algorithm**.**

Secondly, EHD had used for extract the characteristics of training dataset, and decision tree classifier is employed in the classification phase where the feature had been extracted from the test image and then matched with the feature vectors of the training image that has saved, after all the decision has made for content of the test image either normal or non-normal vault the complete system see Figure 3.13.

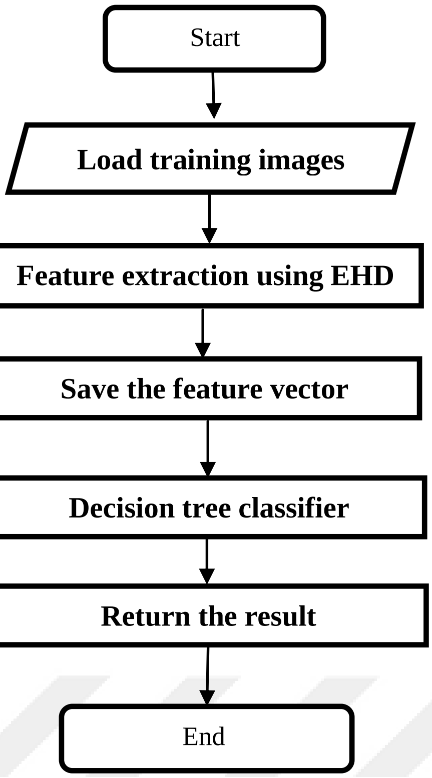

Figure 3.13. Flowchart For EHD With Decision Tree Algorithm**.**

Thirdly, CLD is used here for extract the feature of the training dataset images for using it in the next phase for matching with the input test image, Naïve Bayes classifier is used to classify the content of the test image as shown Figure 3.14.

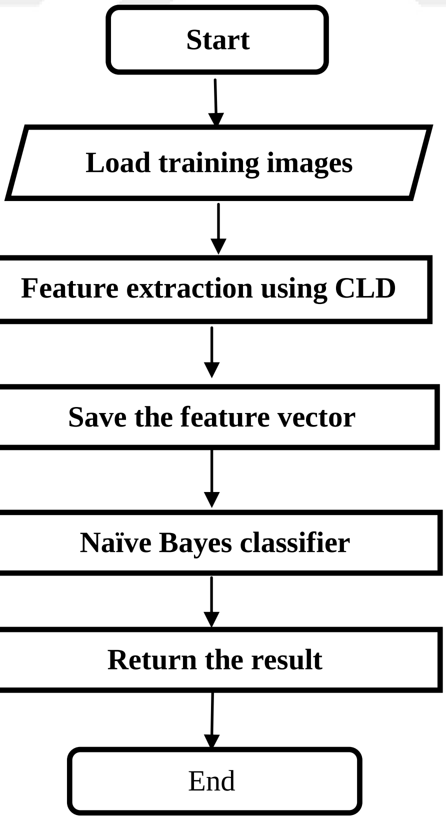

Figure 3.14. Flowchart for CLD with Naïve Bayes classifier algorithm.

Finally, the decision tree classifier had used for classifying the content of the test image, and the descriptor was CLD where it had employed for sets the specific feature from the training images to excel file which is used for matching purpose see Figure 3.15.

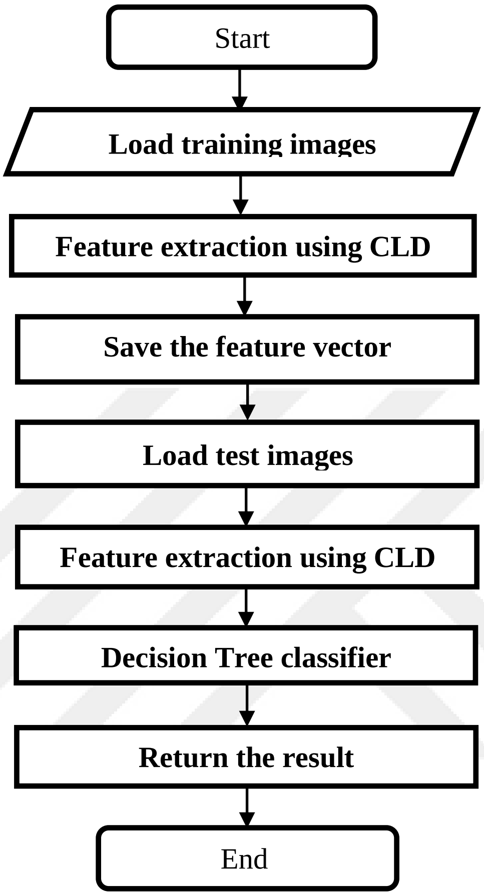

Figure 3.15. Flowchart For CLD With Decision Tree Classifier Algorithm**.**

3.2.2 Experiment 2: A 3-states hidden markov model

The system has built in two phases, features are extracted in the first phase from the input images and these features passed to the 3-state, HMM to be recognized in which class is belong to. The idea behind this system is to handling the image as its contents of three blocks. Obviously, the vault image contents the anterior chamber region, the crystalline lens region, and the ICL lens region as shown in Figure 3.16. Therefore, it can easily modeled by a 3-state hidden Markov model.

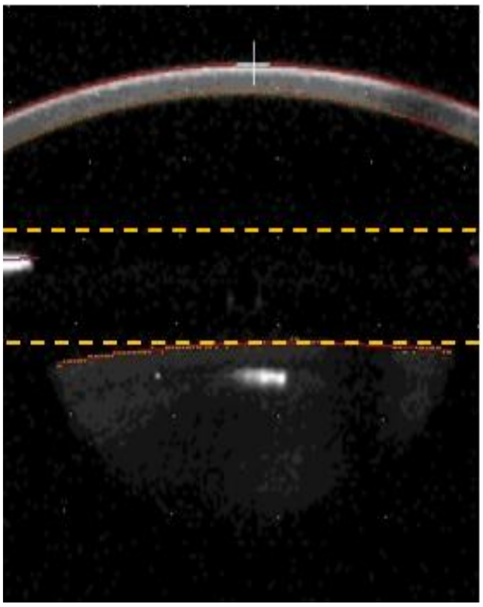

Figure 3.16. Three regions of vault image.

3.2.2.1 Extraction features from image

The input image is converted into grayscale image, in order to gain more speed for execution time the image is resized into width equal to 66 and height 26, the sequence of blocks is generated by overlapping the blocks with height equal to 5 with the same width, the block slides from top to bottom, the overlapping size is only one pixel to down, therefore the total number of blocks is calculated by equation below.

$$N = \frac{Height - Block\ hieght}{Block\ height - overlapping\ size} + 1 \qquad (3.14)$$

In our case here the total number of blocks for each image is equal to 22 blocks, where.

$$N = \frac{26-5}{5-4} + 1 = 22 \qquad (3.15)$$

Now the system has 22 blocks with size 5 x 26 from the input image, from those blocks the feature must extract, the singular value decomposition (SVD) has employed to convert the set of blocks to set of features, it is an essential method for analyzing the data; (Golub, G. H and Reinsch, C., 1970), it is a suitable tool to obtain a useful feature from multivariate data; (Tamayo, Palestinian et al., 1999). The decomposition equation is.

$$X = USV^T \tag{3.16}$$

Where, U is an m × n matrix, S is an n × n diagonal matrix, and V^T is also an n × n matrix, after getting these matrices the single value has taken from each one, therefore, U(1, 1), S(1, 1) and V(2, 2) are saved to be used, which they showed the best performance of the system, the value U(1, 1), S(1, 1) and V(2,2) are quantized into 18, 10, 7 levels, respectively; first value between 0 and 17, second between 0 and 9, and the third is between 0 and 6, finally one value is produced from these three by possible combination, the maximum number of the combination is 1260, therefore each bock has only one value that means for each image generates a vector with size 1 x 22 see Figure 3.17.

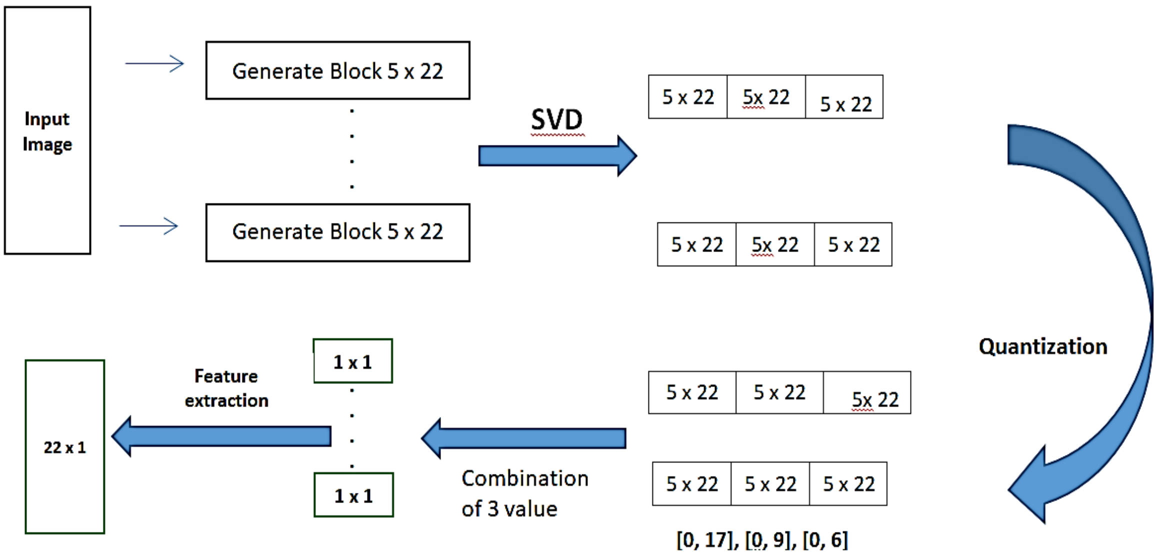

Figure 3.17. Feature extraction.

Finally, the feature vector is produced to be as input to the next phases, which is 3-state HMM.

3.2.2.2 A 3-States hidden markov model

The input image contents three regions anterior chamber, ICL lens, and crystalline lens, that it represents the sequence of events, therefore it is possible to construct the HMM, if the image scan from up to bottom, states always start with anterior chamber, then will transition into ICL lens, and the final transition is to crystal lens, therefore the probability to transition from the anterior chamber to CL lens is 0.5 and probability to stay in the same state is also 0.5, at the same time the state is always crystal lens, that means the state will not change, consequently, the transition probability is equal to 1, from these we can construct the transition matrix as shown below.

The initial state probability of this model is like as following

$$B = \begin{array}{r} \\ Anterior\,Chamber(AC) \\ Crystal\,lens(CL) \\ ICL\,lens \end{array} \begin{array}{c} \begin{array}{ccc} \mathbf{AC} & \mathbf{CL} & \mathbf{ICL} \end{array} \\ \begin{bmatrix} 0.5 & 0.5 & 0 \\ 0 & 0.5 & 0.5 \\ 0 & 0 & 1 \end{bmatrix} \end{array}$$

Figure 3.18. Transition Matrix.

$$\pi = \begin{array}{c} \begin{array}{ccc} \mathbf{AC} & \mathbf{ICL} & \mathbf{CL} \end{array} \\ \begin{bmatrix} 1 & 0 & 0 \end{bmatrix} \end{array}$$

Figure 3.19. Initial Matrix.

Now remaining only the matrix of A, as mentioned above each block will generate a number between 0 and 1260, therefore the A matrix can simply be as below.

$$A = \begin{array}{r} \\ AC \\ ICL \\ CL \end{array} \begin{array}{c} \begin{array}{cccc} 1 & 2 & \ldots & 1260 \end{array} \\ \begin{bmatrix} 1 & 1 & \cdots & 1 \\ \vdots & & \vdots & \vdots \\ 1 & 1 & \cdots & 1 \end{bmatrix} \end{array}$$

Figure 3.20. Probability Matrix.

Having π, A, and B matrices so, it is ready to generate HMM. After finishing the generating data stage, the implementation starts with training the data, which is ready to enter this part of the system, that are used to training HMM see Figure 3.21.

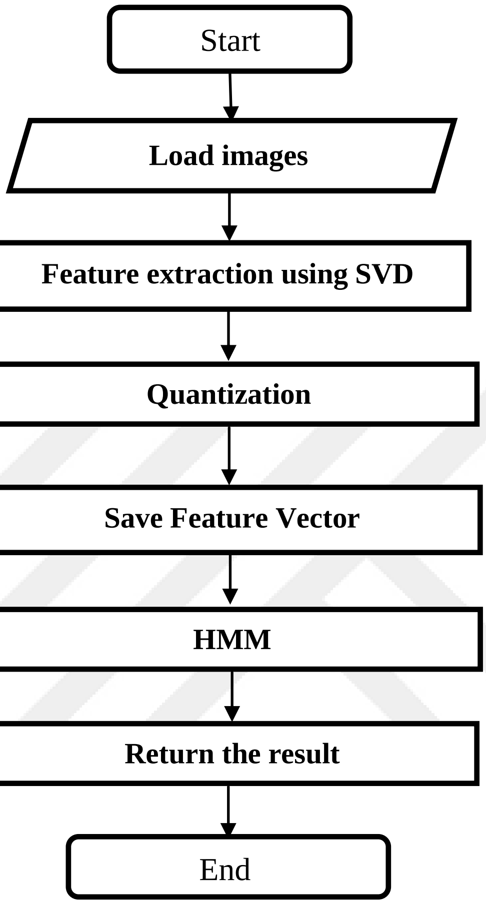

Figure 3.21. Flowchart for SVD with HMM algorithm.

4. RESULTS AND DISCUSSION

4.1 Results

In this thesis the value of the vault estimation has been proposed by exploit the machine learning algorithms, in the first experiment the EHD and CLD have utilized to extract the features of input image individually, the vector of the features could be passed to DT and Naïve Bayes classifiers in order to categorize the image under the study to a specific class, after all, the accuracy of the classification is calculated using a leave-one-out strategy, which is summarized by kept one image from the dataset as a test and leave the others for training and the accuracy is calculated, in the next phase choose the another different image and leave the rest as training with calculating the new accuracy, the experiment repeated N times where N is the total number of images in the dataset, finally, the average of the accuracy of all N time is calculated as the final result. This experiment has simulated using dot net programming (C#) software; this software provides suitable tools for applying such algorithms. A graphics users interface (GUI), it builds to be an interface to the system and to be easier for a user to interact with the program efficiently, consequently achieve the objective of the system. (GUI) is the designs with several buttons see Figure 4.1 that help to select the specific process (method) such as select the EHD for extract feature from the dataset and Naïve Bayes for the classification task.

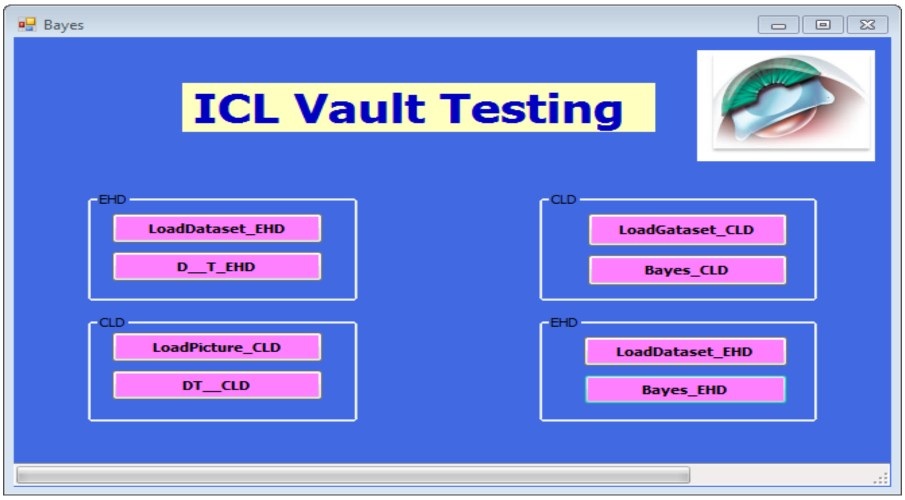

Figure 4.1. GUI window.

The accuracy and efficiency of the proposed algorithms were considered by applying these algorithms on some datasets to obtain the accuracy desired This was done by applying the following equations.

$$Precision_{(i)} = \frac{\text{Total images } classified \text{ correctly }_{(i)}}{\text{Total images tested}} * 100 \qquad (4.1)$$

First of all, the descriptor button will show the user the open file dialog that gives the user area to choose the interested dataset for training the system for both descriptors CLD and EHD, as shown in Figure 4.2, the dataset must be saved in one folder that contains both normal and non-normal vaults dataset folders which should be saved in the folder that is content two separate folders.

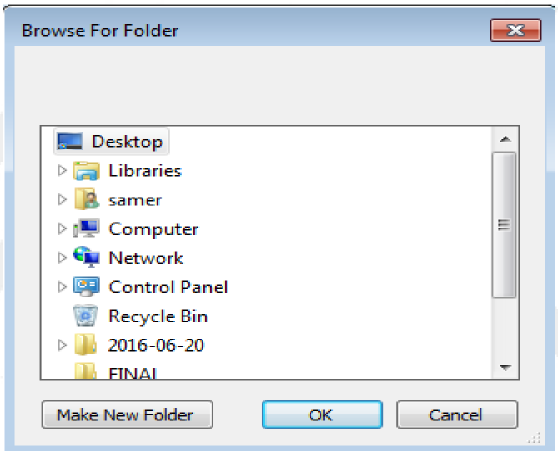

Figure 4.2. Enter dataset window**.**

After training the dataset and extraction of the features from images in a spatial domain, the test image could be selected as in Figure 4.3. to be classified using the Naïve Bayes or DT classifier.

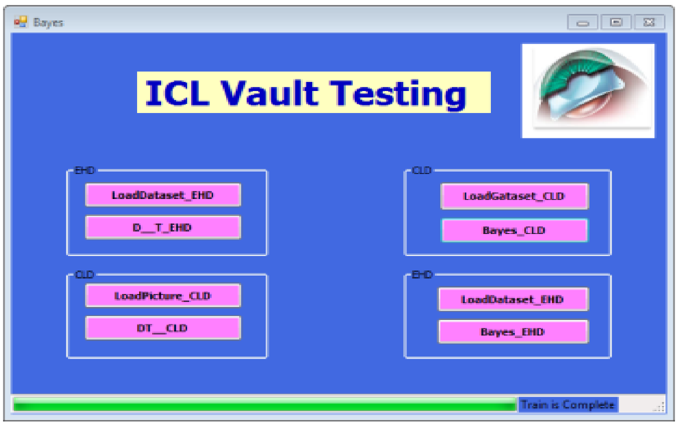

Figure 4.3. Training dataset.

Finally, the result comes out to demonstrate the class which the test image belongs.

After the process operation finished, the result display to the user as a new window content message tells the user about the class that the test image belongs to see Figure 4.4.

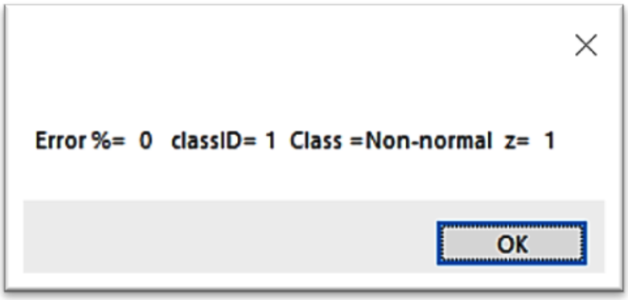

Figure 4.4. Display result**.**

Worthy, to mention the results as a vector of features represented as a number on the Microsoft Excel sheets, which saved in a given direction, here we show some of these data, see Figure 4.5.

0	1	2	3	4	5	6	7	8
0	0.190988	0.011235	0	0.112346	0	0.212468	0.024996	0.012498
0	0.292099	0.044938	0	0.101111	0	0.292099	0.044938	0.011235
0	0.280864	0.011235	0	0.089877	0.012656	0.240469	0.037969	0.012656
0	0.316406	0.063281	0.012656	0.050625	0.012656	0.278438	0.037969	0.012656
0.022469	0.280864	0.022469	0.033704	0.134815	0.012656	0.354375	0.012656	0.012656
0	0.349947	0.049992	0.037494	0.124981	0.014082	0.39429	0.042245	0.014082
0	0.26963	0.033704	0	0.044938	0	0.280864	0.033704	0.011235
0	0.380208	0.042245	0.014082	0.056327	0	0.422454	0.028164	0
0	0.352045	0.056327	0	0.028164	0	0.39429	0.014082	0
0	0.449931	0.037494	0	0.024996	0	0.408372	0.014082	0
0	0.247686	0.055041	0	0.119256	0.0202	0.3636	0.0202	0.0101
0	0.1717	0.0303	0	0.1212	0.0101	0.1717	0	0.0101
0	0.312452	0.024996	0	0.137479	0.014082	0.295718	0.042245	0.014082
0.0101	0.303	0.0202	0	0.0909	0.0202	0.3434	0.0404	0.0101
0.087487	0.412437	0.099985	0.074989	0.287456	0.070409	0.408372	0.070409	0.084491
0.061218	0.346903	0.091827	0.081624	0.418325	0.112233	0.397919	0.091827	0.081624
0	0.266033	0.082562	0.036694	0.110083	0.027521	0.302727	0.036694	0.009174
0.063281	0.341719	0.088594	0.10125	0.316406	0.086939	0.362245	0.057959	0
0.06896	0.301702	0.06034	0.05172	0.206881	0.06034	0.284462	0.00862	0.02586
0.063281	0.341719	0.050625	0.075938	0.189844	0.057959	0.333265	0.01449	0
0	0.187471	0.06249	0.012498	0.06249	0	0.337963	0.014082	0
0.112346	0.24716	0.112346	0.101111	0.235926	0.049992	0.337449	0.06249	0.024996
0	0.177188	0.037969	0	0.126563	0	0.309799	0.028164	0.014082
0.12358	0.24716	0.101111	0.112346	0.258395	0.049992	0.337449	0.087487	0.024996
0	0.2727	0.0202	0	0.1111	0	0.303333	0.011235	0.011235
0.011235	0.235926	0.022469	0.011235	0.067407	0	0.292099	0.011235	0
0	0.2525	0.0202	0.0101	0.0808	0	0.314568	0	0
0.040812	0.3367	0.091827	0.020406	0.23467	0.061218	0.326497	0.020406	0.051015
0	0.26963	0.044938	0	0.067407	0.022469	0.314568	0	0
0.033704	0.325802	0.056173	0.044938	0.224691	0.063281	0.354375	0.025313	0.012656
0	0.312452	0.012498	0	0.037494	0	0.337963	0.014082	0.014082
0	0.238512	0.018347	0	0.064215	0	0.255076	0.020406	0.010203
0	0.24716	0.022469	0	0.056173	0	0.30375	0.012656	0.012656
0.087487	0.362445	0.06249	0.06249	0.187471	0.074989	0.32495	0.012498	0.049992
0.081624	0.357106	0.051015	0.030609	0.285685	0.034478	0.367769	0.103435	0.011493
0.034478	0.310305	0.057464	0.057464	0.356276	0.034478	0.390754	0.068957	0.034478
0.011235	0.280864	0.022469	0	0.044938	0	0.30375	0.025313	0

Figure 4.5. Features in excel file.

Consequently, after the all N time executions on the dataset, the last accuracy for each classifier has been calculated, by investigation the proposed system, the result showed that the Naïve Bayes classifier with CLD is producing higher classification accuracy than the respective of rest components of the system as summarized in Table 4.1.

Table 4.1. Accuracy percentage (%).

Classifier / Descriptor	EHD	CLD
Naïve Bayes	**65**	**85.9**
Decision Tree	**54.6**	**66.6**

The average time required for investigate subsystem on dataset calculated to show the execution time for each algorithm, the result shows that achieve Naïve Bayes with EHD is to spend less time for both training and classification tasks. This is due to the capability of the classifier to dealing with huge amount of data via limited time (Table 4.2.). It also can be concluded that in general, the time for training the naïve Bayes classifier is less than the time spent on training the DT classifier.

Table 4.2. Excecution Time (sec.).

Classifier / Descriptor	EHD	CLD
Naïve Bayes	**0.12**	**0.23**
Decision Tree	**0.34**	**0.54**

A GUI has also been created for implement the second experiment using Matlab R2014a in order to facilitate the procedure of execution, that it contains many taps such as generate a database, load database, training, calculating recognition rate and exit tabs see Figure 4.6. The results of classification for each testing phase and the total accuracy is displayed on the Matlab command window.

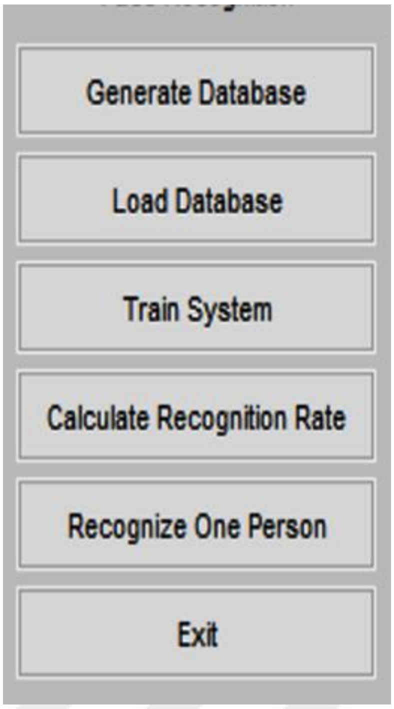

Figure 4.6. GUI tabs.

Dataset is by dividing it into two classes, one for normal vault value that has 40 images for training and the second is a class with non-normal vault value that have also 40 images for training.

Testing stage content 39 images for each class, the recognition process is applied to these images, The strategy that is followed to training and testing dataset is by multi-phases validate, which in the first phase, 40 images for both normal and non-normal dataset for training and 39 images for testing, could be set to the system to measure the accuracy, the accuracy computed by using equation 2.4, the second phase starts with another set of training and testing images, where five of the testing images swapped with five from training images and the accuracy is calculated again, and so on that produce 49 phases.

$$Accuracy = \frac{Correctly\ recognized\ images}{Total\ testing\ images} \qquad (4.2)$$

The accuracies are recorded and the average of accuracies of propose system is calculated, which was 86.113 % that are summarized in Table 3.4.

Table 4.3. Accuracies for all testing stages (%).

Stage Number	Accuracies	Stage Number	Accuracies	Stage Number	Accuracies
1	93.103	18	79.299	35	81.102
2	87.931	19	82.758	36	87.921
3	87.953	20	87.452	37	86.109
4	89.655	21	72.413	38	81.013
5	82.758	22	84.491	39	91.379
6	84.482	23	91.380	40	96.561
7	94.827	24	89.655	41	79.103
8	93.104	25	79.410	42	83.333
9	86.206	26	79.391	43	80
10	87.911	27	79.333	44	85
11	86.291	28	86.207	45	81.666
12	89.663	29	75.662	46	88.333
13	91.299	30	81.034	47	91.667
14	84.480	31	87.941	48	90
15	93.112	32	93.103	49	85
16	96.551	33	81.010	Total Accracy	87.311
17	89.665	34	81.034		

On the other hand, the reason for using Matlab R2014a to simulate the experiment two, which provides a role for implementing the HMM algorithm and suitable to dealing with matrices and extract the useful information through applying singular decomposition value as well as it is robust for dealing with multi-block of sub-images via less time. The time spent for each stage including training the system and testing did not exceed 0.4 seconds for all dataset through investigation of all phases individually as summarized in Table 4.4.

Table 4.4. Code run time(second)**.**

Stage number	Function			Stage number	Function		
	Training	Testing	System		Training	Testing	System
1	28.775	0.775	38.852	26	28.238	0.854	38.885
2	27.547	0.223	39.225	27	28.987	0.558	38.455
3	26.356	0.745	37.852	28	28.778	0.765	38.582
4	27.963	0.852	41.321	29	28.776	0.687	38.922
5	28.542	0.966	38.745	30	28.756	0.958	38.961
6	26.744	0.987	37.123	31	28.225	0.969	38.775
7	28.124	0.785	38.856	32	28.745	0.864	38.965
8	28.889	0.953	37.996	33	28.214	0.886	38.966
9	28.951	0.883	37.957	34	28.365	0.759	38.654
10	28.125	0.238	37.885	35	28.665	0.756	38.325
11	25.115	0.874	38.558	36	28.943	0.778	38.885
12	28.214	0.652	39.614	37	28.976	0.928	38.788
13	28.885	0.552	39.225	38	28.467	0.935	38.796
14	28.337	0.874	37.541	39	28.482	0.699	38.856
15	29.741	0.784	37.365	40	28.534	0.831	38.994
16	29.552	0.897	37.951	41	28.976	0.819	38.865
17	29.423	0.981	40.237	42	28.348	0.763	38.943
18	29.365	0.889	38.923	43	28.882	0.698	38.235
19	27.748	0.754	38.325	44	28.359	0.699	38.885
20	26.658	0.574	38.953	45	28.959	0.866	38.854
21	27.632	0.892	38.761	46	28.559	0.826	38.813
22	27.123	0.884	37.349	47	28.791	0.998	38.922
23	27.356	0.879	37.764	48	28.346	0.739	38.934
24	28.855	0.894	39.462	49	28.973	0.731	38.763
25	28.966	0.853	39.445				

4.2 Discussion

The recognition among such images is still a big challenge because of the similarity between the images that have a normal value of vault and the others with the non-normal value of vault. In terms of accuracy, the results presented in Tables 4.1., indicates that the performance of Naïve Bayes was better than Decision Tree classifier, because the features of each image that have tested compared with all the features of the trained image in the Naïve Bayes method, whereas, the system has compared less than half of the trained features in the Decision Tree method. Therefore, the precision of Naïve Bayes annotation was higher. The content of the images that tested using EHD descriptor was retrieved wrongly; because of the similarity of the image content in both partitions the normal and non-normal vault, where the differences are tiny, that the classifier cannot recognize them clearly. CLD uses the colors feature of the images; therefore, it is evident that by using this descriptor with the Naive Bayes classifier gives the result more accurately than using it with the DT classifier. CLD with Naive Bayes classifier gives the system power to recognize the normal vault images from another, which makes it gives efficiency satisfactory performance, but it could not reach 100% accuracy because some images from different classes have a similarity of subject colors that produce weakness in system performance.

On the other hand, executing time of the system using Naïve Bayes classifier was better in comparison with Decision Tree classifier, because the calculation process for information gain in C4.5 algorithm involved the computing of log function, and the time consuming of the log function is causes a problem on total computation time.

Navigation experiment two did not gives a very high accuracy, the reason behind that is the low rate of differences between the images that contain the normal vault and non-normal vault value, This is sufficient evidence that the problem of measuring the vault remains a major challenge and remaining on the research table. While the model with the HMM was able to recognize about 87.3% off total images, the give precise evidence that the system that had built was performing efficiently for recognition the images.

5. CONCLUSION AND RECOMMENDATIONS

5.1 Conclusion

In this thesis, a system has been proposed to predict the vault posterior by using different methods such as EHD and CLD for extracting the characteristics of the images, as well as Naïve Bayes and decision tree to classify the input image into normal or non-normal class.

Retrieve the content of the image strongly is depend on many factors, such as, extracting the characteristic of the image efficiently, selecting the suitable descriptor which is built on the basis of the nature of the image content, the classifier capability for dealing with the descriptors outputs as well as with dataset, in order to achieve efficient classification performance, and finally, capability to defeat the challenge that is caused by the differences between the concept of high level feature represented by semantic concepts and low level feature of the image which is represented by color texture, shape and spatial layout. This work summarized that by building a smart algorithm mainly to dealing with texture and color based features, are the strengths to improve the precision, lessen annotation executing time, growth system competence, decrease the dimensions of the feature vector, and increase training quickness.

5.2 Recommendation

In order to develop the diagnosis of the medical state more accurately and efficiently, it is vital to adopt a larger database in order to extract the features of images more efficiently, in addition to relying on other factors in addition to the factors used in this research such as measuring the basement or white to white in addition to using other descriptors related to extracting the texture image like Scale-invariant feature transform descriptor (SIFT) or Speeded-Up Robust Features (SURF), in order to help the classifier to distinguish between successful and unsuccessful operation more efficiently and accurately.

REFERENCES

Alahi, A., Ortiz, R., and Vandergheynst, P., 2012. Freak: Fast retina keypoint. In 2012, IEEE Conference on Computer Vision and Pattern Recognition,pp. 510-517.

Alfonso, J. F., Fernandez-Vega, L., Lisa, C., Fernandes, P., González-Meijome, J., and Montés-Micó, R.,2012. Long-term evaluation of the central vault after phakic Collamer lens ICL implantation using OCT. Graefe's Archive for Clinical and Experimental Ophthalmology, 250, 12, 1807-1812.

Alfonso, J. F., Fernández-Vega, L., Lisa, C., Fernandes, P., Jorge, J., and Micó, R. M., 2012. Central vault after phakic intraocular lens implantation, correlation with anterior chamber depth, white-to-white distance, spherical equivalent, and patient age. Journal of Cataract and Refractive Surgery, 38, 46-53.

Alfonso, J. F., Lisa, C., Abdelhamid, A., Fernandes, P., Jorge, J., and Montés-Micó, R., 2010. Three-year follow-up of subjective vault following myopic implantable Collamer lens implantation. Graefe's Archive for Clinical and Experimental Ophthalmology, 248, 12, 1827-1835.

Alfonso, J. F., Lisa, C., Palacios, A., Fernandes, P., González-Méijome, J. M., and Montés-Micó, R., 2009. Objective vs subjective vault measurement after myopic implantable collamer lens implantation. American journal of ophthalmology, 147, 6, 978-983.

Apte, C., 2010. Business optimization. In Proceedings of the 27th International Conference on Machine Learning ICML-10, 1-2.

Auda, G., and Kamel, M., 1999. Modular neural networks, a survey. International Journal of Neural Systems, 9, 129-151.

Bachmann M, Ullrich S, and Thiel MJ., 2002. Imaging of posterior chamber phakic intraocular lens by optical coherence tomography. Cataract Refract Surg; 28, 360–363.

Bagirov, A. M., 2008. Modified global k-means algorithm for minimum sum-of-squares clustering problems. Pattern Recognition, 41, 10, 3192-3199.

Barkana, Y., Gerber, Y., Elbaz, U., Schwartz, S., Ken-Dror, G., Avni, I., and Zadok, D., 2005. Central corneal thickness measurement with the Pentacam Scheimpflug system, optical low-coherence reflectometry pachymeter, and ultrasound pachymetry. Journal of Cataract and Refractive Surgery, 31, 9, 1729-1735.

Barros, R. C., De Carvalho, A. C., and Freitas, A. A., 2015. Automatic design of decision-tree induction algorithms. Germany: Springer International Publishing.

Bhatia, S., 2014. A new improved technique for initial cluster centers of K means clustering using the Genetic Algorithm. In Convergence of Technology I2CT, 1-4.

Blasch, E., Chen, Y., Chen, G., Shen, D., and Kohler, R., 2014. Information fusion in a cloud-enabled environment. In High-Performance Cloud Auditing and Applications 91-115, Springer, New York, NY.

Blasch, E., Steinberg, A., Das, S., Llinas, J., Chong, C., Kessler, O. and White, F., 2013,. Revisiting the JDL model for information Exploitation. In Information Fusion, 129-136.

Bober, M., 2001. MPEG-7 visual shape descriptors. IEEE Transactions on circuits and systems for video technology, 11, 6, 716-719.

Boczar, T., 2001. Identification of a specific type of PD from acoustic emission frequency spectra. IEEE Transactions on Dielectrics and Electrical Insulation, 8, 4, 598-606.

Boser, B. E., Guyon, I. M., and Vapnik, V. N., 1992. A training algorithm for optimal margin classifiers. In Proceedings of the fifth annual workshop on Computational learning theory, 144-152.

Bradley, P. S., and Fayyad, U. M., 1998,. Refining Initial Points for K-Means Clustering, in ICML 98, 91-99.

Braun, A. C., Weidner, U., and Hinz, S., 2011, Support vector machines, import vector machines and relevance vector machines for hyperspectral classification—A comparison. InHyperspectral Image and Signal Processing: Evolution in Remote Sensing (WHISPERS), 3rd Workshop on, 1-4.

Brown, M., and Süsstrunk, S., 2011, Multi-spectral SIFT for scene category recognition. In Computer Vision and Pattern Recognition (CVPR), 2011 IEEE Conference on, 177-184.

Burghouts, G. J., and Geusebroek, J. M., 2009. Performance evaluation of local color invariants. Computer Vision and Image Understanding, 113, 1, 48-62.

Bylsma S.S, Zalta AH, Foley E, Osher RH., 2002. Phakic posterior chamber intraocular lens pupillary block. J Cataract Refract Surg 28:2222 – 2228.

Calonder, M., Lepetit, V., Strecha, C., and Fua, P., 2010, September. Brief: Binary robust independent elementary features. In European conference on computer vision, 778-792. Springer, Berlin, Heidelberg.

Chang JS, Meau AY, 2007 Visian Collamer phakic intraocular lens in high myopic Asian eyes. J Refract Surg 17 – 25.

Chen, X., Miao, H., Naidu, R. K., Wang, X., and Zhou, X., 2016. Comparison of early changes in and factors affecting vault following posterior chamber phakic implantable Collamer lens implantation without and with a central hole (ICL V4 and ICL V4c). BMC Ophthalmology, 16, 1, 161.

Choi KH, Chung SE, Chung TY, Chung ES, 2007., Ultrasound biomicroscopy for determining Visian implantable contact lens length in phakic IOL implantation. J Refract Surg 23, 362 – 367.

Chung TY, Park SC, Lee MO, Ahn K, Chung ES, 2009 Changes in iridocorneal angle structure and trabecular pigmentation with STAAR implantable Collamer lens during 2 years. J Refract Surg 25, 251 – 258.

Cui, Q., Bai, F. S., Gao, B., and Liu, T. Y., 2015,. Global optimization for advertisement selection in sponsored search. Journal of Computer Science and Technology, 30(2), 295-310.Dalal, N., and Triggs, B. 2005,. Histograms of oriented gradients for human detection. In Computer Vision and Pattern Recognition, CVPR 2005. IEEE Computer Society Conference on, 886-893.

Du, G. P., Huang, Y. F., Wang, L. Q., Wang, D. J., Guo, H. L., Yu, J. F., ... and Huang, H. B., 2012. Changes in objective vault and effect on vision outcomes after implantable Collamer lens implantation: 1-year follow-up. European journal of ophthalmology, 22, 2, 153-160.

Dubbelman, M., and Van der Heijde, G. L., 2001. The shape of the aging human lens: curvature, equivalent refractive index and the lens paradox. Vision Research, 41, 1867-1877.

Duda, R. O., Hart, P. E., and Stork, D. G., 2012., Pattern Classification. John Wiley and Sons.

Eddy, S. R., 1996. Hidden Markov models. Current opinion in structural biology, 6, 3, 361-365.

Eissa, S. A., Sadek, S. H., and El-Deeb, M. W. , 2016. Anterior chamber angle evaluation following phakic posterior chamber Collamer lens with CentraFLOW and its correlation with ICL vault and intraocular pressure. Journal of Ophthalmology.

El Meslouhi, O., Allali, H., Gadi, T., Benksddour, Y. A., and Kardouchi, M.,2010. Image registration using the opponentSIFT descriptor: Application to colposcopic images with specular reflections. In Signal-Image Technology and Internet-Based Systems (SITIS), Sixth International Conference, 12-17.

Elies D, Coret A, Puig J, Rombouts A. Protocolos en el implante de lentes fáquicas tipo ICL. Annals d’Oftalmologia 2004; 30–34.

Ermini, L., Catani, F., and Casagli, N., 2005. Artificial neural networks applied to landslide susceptibility assessment.Geomorphology, 66, 1-4, 327-343.

Friedman, N., Geiger, D., and Goldszmidt, M., 1997. Bayesian network classifiers. Machine learning, 29, 131-163.

Garcia, V., Debreuve, E., and Barlaud, M., 2008. Fast k nearest neighbor search using GPU. IEEE Computer Society Conference on Computer Vision and Pattern Recognition Workshops, 1-6.

Garcia-De la Rosa, G., Olivo-Payne, A., Serna-Ojeda, J. C., Salazar-Ramos, M. S., Lichtinger, A., Gomez-Bastar, A. and Graue-Hernandez, E. O., 2017. Anterior segment optical coherence tomography angle and vault analysis after toric and non-toric implantable Collamer lens V4c implantation in patients with high myopia. British Journal of Ophthalmology.

Ghoreishi, M., and Mohammadinia, M., 2014. Correlation between preoperative sizing of implantable Collamer lens (ICL) by white-to-white and sulcus-to-sulcus techniques, and postoperative vault size measured by Scheimpflug imaging. J Clin Exp Ophthalmol, 5, 4, 351.

Golub, G. H., and Reinsch, C., 1970. Singular value decomposition and least squares solutions. Numerische mathematik, 14, 5, 403-420.

Gonvers, M., Bornet, C., and Othenin-Girard, P., 2003. Implantable contact lens for moderate to high myopia: relationship of vaulting to cataract formation. Journal of Cataract and Refractive Surgery, 29, 5, 918-924.

Gonzalez-Lopez, F., Mompean, B., Bilbao-Calabuig, R., Vila-Arteaga, J., Beltran, J., and Baviera, J., 2018. Dynamic Assessment of light-induced Vaulting changes of implantable collamer lens with central port by Swept-Source OCT: Pilot Study. Translational vision science and technology, 7, 3, 4-4.

Grewal, D., Jain, R., Brar, G. S., and Grewal, S. P. S., 2008. Pentacam tomograms: a novel method for quantification of posterior capsule opacification. Investigative ophthalmology and visual science, 49, 5.

Grewal, S. P. S., Jain, R., Gupta, R., and Grewal, D., 2006. Role of Scheimpflug imaging in traumatic intralenticular foreign body. American journal of ophthalmology, 142, 4, 675-676.

Guell JL, Morral M, Kook D, Kohnen T., 2010. Phakic intraocular lenses part 1: historical overview, current models, selection criteria, and surgical techniques. J Cataract Refract Surg. 36, 1976 – 1993.

Guo, X., and Cao, X., 2012. MIFT: A framework for feature descriptors to be mirror reflection invariant. Image and Vision Computing, 30, 8, 546-556.

Haralick, R. M., 1976. The table look-up rule. Communications in Statistics-Theory and Methods, 5, 12, 1163-1191.

Jain, A. K., 1989. Fundamentals of digital image processing. Englewood Cliffs, NJ; Prentice Hall.

Jain, A. K., Duin, R. P. W., and Mao, J., 2000. Statistical pattern recognition: A review. IEEE Transactions on pattern analysis and machine intelligence, 22, 1, 4-37.

Jain, R., and Grewal, S. P. S., 2009. Pentacam: principle and clinical applications. Journal of Current Glaucoma Practice, 3, 2, 20-32.

Jin, Z. J., Qian, H., and Zhu, M. L., 2010. Gaussian processes in inverse reinforcement learning. In Machine Learning and Cybernetics (ICMLC), 2010 International Conference on 225-230.

Johnson, R. B., and onwuegbuzie, A. J., 2004. Mixed methods research; a research paradigm whose time has come. Educational researcher, 33, 7, 14-26.

Jolliffe, I., 2011. Principal component analysis. In International encyclopedia of statistical science, 1094-1096. Springer, Berlin, Heidelberg.

Juang, B. H., Levinson, S., and Sondhi, M., 1986. Maximum likelihood estimation for multivariate mixture observations of Markov chains corresp. IEEE Transactions on Information Theory, 32, 2, 307-309.

Kabbai, L., Azaza, A., Abdellaoui, M., and Douik, A., 2015,. Image matching based on LBP and SIFT descriptor. In systems, signals and devices (SSD), 2015 12th International Multi-Conference, 1-6.

Kachalsky, I., Zakirzyanov, I., and Ulyantsev, V., 2017. Applying Reinforcement Learning and Supervised Learning Techniques to Play Hearthstone. In Machine Learning and Applications, 16th IEEE International Conference, 1145-1148.

Kamiya, K., Shimizu, K., and Kawamorita, T., 2009. Changes in vaulting and the effect on refraction after phakic posterior chamber intraocular lens implantation. Journal of Cataract and Refractive Surgery, 35, 9, 1582-1586.

Kamiya, K., Shimizu, K., Ando, W., Igarashi, A., Iijima, K., and Koh, A., 2015. Comparison of the vault after implantation of posterior chamber phakic intraocular lens with and without a central hole. Journal of Cataract and refractive Surgery, 41, 1, 67-72.

Kasutani, E., and Yamada, A., 2001. The MPEG-7 color layout descriptor: a compact image feature description for high-speed image/video segment retrieval. In Image Processing, 2001. Proceedings. International Conference, 1,674-677.

Kim, W. K., Cho, E. Y., Kim, H. S., and Kim, J. K., 2013. The analysis of vault change after posterior chamber phakic intraocular lens size exchange. Journal of the korean ophthalmological society, 54, 11, 1669-1674.

Kim, W. K., Cho, E. Y., Kim, H. S., Kim, D. S., and Kim, J. K, 2013. The benefits of one day, one eye surgery in bilateral ICL implantation. Journal of the korean ophthalmological Society, 54, 7, 1019-1024.

Kim, W. K., Ryu, I. H., Kim, J. K., and Yang, H., 2012. Effects of transient prone position on vault and anterior chamber angle in ICL implanted patients. Journal of the korean ophthalmological Society, 53, 6, 761-766.

Koivula A, Kugelberg M., 2007. Optical coherence tomography of the anterior segment in eyes with phakic refractive lenses ophthalmology; 114, 2031–2037.

Kojima T, Maeda M, Yoshida Y, Ito M, Nakamura T, Hara Israeli, 2010. Posterior chamber phakic implantable Collamer lens: changes in the vault during 1 year. J Refract Surg., 26, 327 – 332.4

Kojima, T., Maeda, M., Yoshida, Y., Ito, M., Nakamura, T., Hara, S., and ichikawa, K.,2010. Posterior chamber phakic implantable Collamer lens: changes in the vault for 1 year. Journal of Refractive Surgery, 26, 5, 327-332.

Kononenko, I., 2001. Machine learning for medical diagnosis: history, state of the art and perspective. Artificial Intelligence in medicine, 23, 1, 89-109.

Kordylewski, H., Graupe, D., and Liu, K., 2001. A novel large-memory neural network as an aid in medical diagnosis applications. IEEE Transactions on Information Technology in Biomedicine, 5, 3, 202-209.

Krogh, A., Larsson, B., Von Heijne, G., and Sonnhammer, E. L., 2001. Predicting transmembrane protein topology with a hidden Markov model; application to complete genomes. Journal of molecular biology, 305, 3, 567-580.

Kumar, R. M., and Sreekumar, K., 2014. A survey on image feature descriptors. computer Science and information technology, 5, 7668-7673.

Kurzyński, M. W., 1983. The optimal strategy of a tree classifier. Pattern Recognition, 16, 1, 81-87.

Kwak, A. Y., Ryu, I. H., Kim, J. K., Kim, T. I., and Ha, B. J., 2012. Effect of preoperative crystalline lens rise on vaulting after implantable Collamer lens implantation. Journal of the Korean Ophthalmological Society, 53, 12, 1749-1755.

Lackner, B., Pieh, S., Schmidinger, G., Simader, C., Franz, C., Dejaco-Ruhswurm, I., and Skorpik, C., 2004. Long-term results of implantation of phakic posterior chamber intraocular lenses. Journal of Cataract and Refractive Surgery, 30, 11, 2269-2276.

Lackner, B., Schmidinger, G., Pieh, S., Funovics, M. A., and Skorpik, C., 2005. Repeatability and reproducibility of central corneal thickness measurement with Pentacam, Orbscan, and ultrasound. Optometry and vision science, 82, 10, 892-899.

Lee, D. H., Choi, S. H., Chung, E. S., and Chung, T. Y., 2012. Correlation between preoperative biometry and posterior chamber phakic visian implantable collamer lens vaulting. Ophthalmology, 119, 2, 272-277.

Lee, H., Kang, D. S. Y., Choi, J. Y., Ha, B. J., Kim, E. K., and Seo, K. Y., 2018. Analysis of pre-operative factors affecting the range of optimal vaulting after implantation of 12.6-mm V4c implantable collamer lens in myopic eyes. BMC Ophthalmology, 18, 1, 163.

Lee, H., Kang, D. S. Y., Ha, B. J., Choi, M., Kim, E. K., and Seo, K. Y., 2015. Effect of accommodation on vaulting and movement of a posterior chamber phakic lenses in eyes with implantable Collamer lenses. American journal of ophthalmology, 160, 4, 710-716.

Lee, H., Kang, S. Y., Seo, K. Y., Chung, B., Choi, J. Y., and Kim, K. S., 2014. Dynamic vaulting changes in V4c versus V4 posterior chamber phakic lenses under differing lighting conditions. American journal of ophthalmology, 158, 6, 1199-1204.

Lewis, D. D., 1998. Naïve Bayes at forty: The independence assumption in information retrieval. In European conference on machine learning, 4-15. Springer, Berlin, Heidelberg.

Li, X., Chen, S. C., Shyu, M. L., and Furht, B., 2002. Image retrieval by color, texture, and spatial information. 8th Inter. Con. on Dis. Multi-Sys., DMS'2002, San Francisco Bay, California, USA, 1-8.

Li, Y., Yang, Q., Lai, S., and Li, B., 2015. A new speculative execution algorithm based on C4. 5 decision tree for Hadoop. In International Conference of Young Computer Scientists, Engineers and Educators, 284-291.

Likas, A., Vlassis, N., and Verbeek, J. J., 2003. The global k-means clustering algorithm. Pattern Recognition, 36, 2, 451-461.

Lindland, A., Heger, H., Kugelberg, M., and Zetterström, C.,2010. Vaulting of my-opic and toric Implantable Collamer Lenses during accommodation measured with Visante optical coherence tomography. Ophthalmology, 117, 6, 1245-1250.

Lindland, A., Heger, H., Kugelberg, M., and Zetterström, C., 2012. Changes in vaulting of myopic and toric implantable Collamer lenses in different lighting conditions. Acta ophthalmologica, 90, 8, 788-791.

Lisa, C., Baamonde, B., Pérez-Vives, C., Montés-Micó, R., and Alfonso, J. F., 2015. Five-year functional outcomes and vault of− 20 diopters myopic phakic intraocular lens implantation. Journal of cataract and refractive surgery, 41, 12, 2724-2730.

Liu, B., Blasch, E., Chen, Y., Shen, D., and Chen, G., 2013,. Scalable sentiment classification for big data analysis using naive Bayes classifier. In Big Data, IEEE International Conferenc, 99-104.

Liu, B., Chen, Y., Blasch, E., Pham, K., Shen, D., and Chen, G., 2014. A holistic cloud-enabled robotics system for real-time video tracking applications. In future information technology, 455-468.

Liu, Z., and Bai, L., 2008. Evaluating the supplier cooperative design ability using a novel support vector machine algorithm. In Computer Supported Cooperative Work in Design, 2008. CSCWD. 12th International Conference, 986-989.

Livingston, F., 2005. Implementation of Breiman's random forest machine learning algorithm. ECE591Q Machine Learning Journal Paper, 1-13.

Lloyd, S.,1982. Least squares quantization in PCM. IEEE transactions on information theory, 28, 2, 129-137.

Lowe, D. G, 1999. Object recognition from local scale-invariant features. In Computer vision, 1999. The proceedings of the seventh IEEE international conference on, 2, 1150-1157.

Lv, H., and Tang, H.,2011. Machine learning methods and their application research. In Intelligence Information Processing and Trusted Computing (IPTC), 2011 2nd International Symposium on, 108-110.

Maeng, H. S., Chung, T. Y., Lee, D. H., and Chung, E. S.,2011. Risk factor evaluation for cataract development in patients with low vaulting after phakic intraocular lens implantation. Journal of Cataract and Refractive Surgery, 37, 5, 881-885.

Manjunath, B. S., Ohm, J. R., Vasudevan, V. V., and Yamada, A., 2001. Color and texture descriptors. IEEE Transactions on circuits and systems for video technology, 11,6, 703-715.

Manjunath, B. S., Salembier, P., and Sikora, T. (Eds.).,2002.Introduction to MPEG-7: multimedia content description interface, 1.

Martens, H. H., 1959. Two notes on machine "Learning". Information and Control, 2, 4, 364-379.

Michalski, R. S., Carbonell, J. G., and Mitchell, T. M. (Eds.)., 2013. Machine learning: An artificial intelligence approach. Springer Science and Business Media.

Miyamoto, E., and Merryman, T., 2005. Fast calculation of Haralick texture features. Human computer interaction institute, Carnegie Mellon university, Pittsburgh, USA.

Mohanaiah, P., Sathyanarayana, P., and GuruKumar, L., 2013. Image texture feature extraction using GLCM approach.International Journal of Scientific and Research Publications, 3, 5, 1.

Mukherjee, S., and Sharma, N., 2012. Intrusion detection using naive Bayes classifier with feature reduction. Procedia Technology, 4, 119-128.

Nguyen, K. A., Zhang, H., and Stewart, R. A., 2013. Development of an intelligent model to categorise residential water end use events. Journal of Hydro-Environment Research, 7, 3, 182-201.

Nigam, V. P., and Graupe, D., 2004. A neural-network-based detection of epilepsy. Neurological Research, 26, 1, 55-60.

Ogle, V. E., and Stonebraker, M., 1995. Chabot; Retrieval from a relational database of images. Computer, 9, 40-48.

Panuccio, A., Bicego, M., and Murino, V., 2002. A Hidden Markov Model-based approach to sequential data clustering. In joint iapr international workshops on statistical techniques in pattern recognition and structural and syntactic pattern recognition, 734-743.

Parveen, P., and Thuraisingham, B., 2012,. Unsupervised incremental sequence learning for insider threat detection. In intelligence and security informatics (isi), IEEE international conference, 141-143.

Pass, G., Zabih, R., and Miller, J., 1997. Comparing images using color coherence vectors. In Proceedings of the fourth ACM international conference on Multimedia, 65-73.

Perner, P. (Ed.)., 2014. Machine learning and data mining in pattern recognition, 10th International Conference, MLDM 2014, petersburg, Russia, 21-24.

Pineda-Fernández, A., Jaramillo, J., Vargas, J., Jaramillo, M., Jaramillo, J., and Galíndez, A., 2004. Phakic posterior chamber intraocular lens for high myopia. Journal of Cataract and Refractive Surgery, 30, 1, 2277-2283.

Portugal, I., Alencar, P., and Cowan, D., 2017. The use of machine learning algorithms in recommender systems: a systematic review. Expert systems with applications.

Quinlan, J. R., 1986. Induction of decision trees. Machine learning, 1, 1, 81-106.

Quinlan, J. R., and Rivest, R. L., 1989. Inferring decision trees using the minimum description lenght principle. Information and computation, 80, 3, 227-248.

Rao, K.M.M., 2007, Deputy Director, NRSA, Hyderabad-500 037, Overview of image processing, readings in image processing.

Redmond, S. J., and Heneghan, C., 2007. A method for initialising the K-means clustering algorithm using kd-trees.Pattern recognition letters, 28, 8, 965-973.

Reinstein, D. Z., Lovisolo, C. F., Archer, T. J., and Gobbe, M., 2013. Comparison of postoperative vault height predictability using white-to-white or sulcus diameter–based sizing for the Visian Implantable Collamer Lens. journal of refractive surgery, 29, 1, 30-35.

Rish, I., 2001. An empirical study of the naive Bayes classifier. In IJCAI workshop on empirical methods in artificial intelligence, 3, 41-46.

Rublee, E., Rabaud, V., Konolige, K., and Bradski, G., 2011. ORB: An efficient alternative to SIFT or SURF. In computer vision (ICCV), 2011 IEEE international conference, 2564-2571.

Russell, S. J., and Norvig, P., 2016. Artificial intelligence, a modern approach. Malaysia; Pearson Education Limited.

Safavian, S. R., and Landgrebe, D., 1991. A survey of decision tree classifier methodology. IEEE transactions on systems, man, and cybernetics, 21, 3, 660-674.

Sanders DR , 2008. Anterior subcapsular opacities and cataracts 5 years after surgery in the Visian implantable Collamer lens FDA trial. J Refract Surg., 24, 566 – 570.

Sarwar, B. M., Karypis, G., Konstan, J. A., and Riedl, J.,2001. Item-based collaborative filtering recommendation algorithms, 1, 285-295.

Schmidinger, G., Lackner, B., Pieh, S., and Skorpik, C., 2010. Long-term changes in posterior chamber phakic intraocular Collamer lens vaulting in myopic patients. Ophthalmology, 117, 8, 1506-1511.

Sikora, T., 2001. The MPEG-7 visual standard for content description-an overview. IEEE Transactions on circuits and systems for video technology, 11, 6, 696-702.

Singha, M., and Hemachandran, K., 2012. Content based image retrieval using color and texture. Signal and Image Processing, 3, 1, 39.

Smallman, D. S., Probst, L., and Rafuse, P. E., 2004. Pupillary block glaucoma secondary to posterior chamber phakic intraocular lens implantation for high myopia. Journal of cataract and refractive Surgery, 30,4, 905-907.

Tabari, H., Zamani, R., Rahmati, H., and Willems, P., 2015. Markov chains of different orders for streamflow drought analysis. Water resources management, 29, 9, 3441-3457.

Tamayo, P., Slonim, D., Mesirov, J., Zhu, Q., Kitareewan, S., Dmitrovsky, Exchange rate and Golub, T. R., 1999. Interpreting patterns of gene expression with self-organizing maps, methods and application to hematopoietic differentiation. Proceedings of the National Academy of Sciences, 96, 6, 2907-2912.

Tan, T. E., Liu, Y. C., Jayasinghe, L. S., and Mehta, J. S., 2017. Intraoperative Optical Coherence Tomography Vault Measurement in Posterior Chamber Phakic Intraocular Lens Implantation. Journal of Refractive Surgery, 33, 4, 274-277.

Taylor, S. J., Bogdan, R., and DeVault, M., 2015. Introduction to qualitative research methods: A guidebook and resource.

Titiyal, J. S., Kaur, M., Sahu, S., Sharma, N., and Sinha, R., 2017. Real-time assessment of intraoperative vaulting in implantable Collamer lens and correlation with postoperative vaulting. European journal of ophthalmology, 27, 1, 21-25.

Van Biesen, W., Sieben, G., Lameire, N., and Vanholder, R., 1998. Application of Kohonen neural networks for the non-morphological distinction between glomerular and tubular renal disease. Nephrology Dialysis transplantation, 13, 1, 59-66.

Van De Sande, K., Gevers, T., and Snoek, C., 2010. Evaluating color descriptors for object and scene recognition. IEEE transactions on pattern analysis and machine intelligence,32, 9, 1582-1596.

Vetter, J. M., Tehrani, M., and Dick, H. B., 2006. Surgical management of acute angle-closure glaucoma after toric implantable contact lens implantation. Journal of Cataract and Refractive Surgery, 32, 6, 1065-1067.

Wu, P., Manjunath, B. S., Newsam, S., and Shin, H. D., 2000. A texture descriptor for browsing and similarity retrieval. Signal processing: Image communication, 16, 1-2, 33-43.

Xie, J., and Jiang, S., 2010, A simple and fast algorithm for global K-means clustering. In Education Technology and Computer Science, second international workshop, 2, 36-40.

Yousef, M., Nebozhyn, M., Shatkay, H., Kanterakis, S., Showe, L. C., and Showe, M. K, 2006. Combining multi-species genomic data for microRNA identification using a Naive Bayes classifier. Bioinformatics, 22, 11, 1325-1334.

Yuan, Y., Song, Q. B., and Shen, J. Y., 2002. Automatic video classification using decision tree method. In machine learning and cybernetics, 2002. Proceedings. 2002 International Conference, 3, 1153-1157.

Zaldivar R, Oscherow S, Piezzi V. Bioptics,. 2003. Our personal experience. In: Probst LE, editor. LASIK Advances, Controversies and Customs. Thorofare, New Jersey, 249–257.

Zhang, M. L., and Zhou, Z. H., 2007. ML-KNN: A lazy learning approach to multi-label learning. Pattern recognition, 40, 7, 2038-2048.

Zhang, S., Huang, J., Huang, Y., Yu, Y., Li, H., and Metaxas, D. N., 2010. Automatic image annotation using group sparsity. In Computer Vision and Pattern Recognition, 3312-3319.

Zheng, Q. Y., Xu, W., Liang, G. L., Wu, J., and Shi, J. T., 2016. Preoperative Biometric Parameters Predict the Vault after ICL Implantation; A Retrospective Clinical Study. Ophthalmic research, 56, 4, 215-221.

Appendix A: published version of the paper.

Appendix A: published version of the paper.

A smart algorithm to predict the post-operative parameters of Intra – corneal lens

Hala Zaid Abdulhameed
Department of Electric Electronic and Computer Engineering,
University of Aksaray

Dr. Nebras Hussein
Biomedical Engineering department, Al-Khawarizmi College of Engineering

Abstract— Lens implantation has become easier than in the past because studies have been conducted to avoid complications when and after the implantation process; the most inevitable approach to avoid ICL difficulties is to accomplish the best possible separation between the back ICL surface and the anterior crystalline lens pole which is called vault in ophthalmology. Recently, machine learning technique is broadly employed in research especially in medical images, due to the ability to analyze a huge amount of data, and also using intelligent methods in order to make the suitable decision which assists physicians in the interpretation the images. To evaluating the postoperative patient eyes status by employing machine learning algorithms, in this work a system has been built that has split into feature extraction and classification parts. edge histogram descriptor (EHD) and color layout descriptor (CLD) have been used for extract the features of the images, Naïve Bayes and decision tree classifire have used for classification, where EHD had employed with classifiers seperetely then the precision has calculated, likewise the CLD has employed with the same two classifiers.

Keywords: Machine learning, feature extraction, Naïve Bayes classifier, Decision Tree classifier, Image retrieval, ICL.

INTRODUCTION

A lots of surgical correction of high myopia has substituted by implantable collamer lens (ICL) implantation due to the successful which has achieved by ICL implantation operations [1, 2], which is made of collamer and can be implanted inside the human eye where it is a flexible and hydrophilic material, collamer is made up of HEMA Hydrogel, water, and porcine collagen [3]. Many researches have confirmed that despite many benefits achieved by lenses for patients by implanting it in his/her eye, but pointed to the postoperative complications in some cases because of the vault (the distance between the posterior surface of the ICL and the anterior surface of the crystalline lens) [4] as shown in Fig. 1, therefore the vault assessment is an essential manner in order to make the implantation more safety and successful procedure [5].

There are several ways to evaluate the vault, in the beginning, vault was measured using traditional technique like slit-lamp which is called subjective method [6 , 7], then after that the vault has been measured objectively by using more recent techniques for instance optical coherence tomography [8, 9]. Subsequently, vault is an aspect key to success the ICL implementation; therefore, it is required to measure the value of the vault accurately and swiftly. Therefor in this paper a smart algorithm has been proposed that used capability of computer and by employed the computer algorithms, methods, and techniques i.e. machine learning techniques and image processing technique.

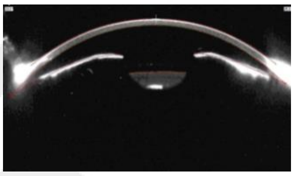

Fig.1 Vault illustration

RELATED WORK

Numerous methods and techniques have been used for measuring and evaluating the vault, which were categorized into various kinds depend on the device used.

Researchers in 2009, by using OTC for measuring the vault [10], and When the vault is very poor (low value), it causes damage to the crystalline lens. This is due to contact the implanted lens with front surface of the crystalline lens, which is lead to cataract formation. After measuring the vault, the values indicate that there is a strong and interconnected relationship between the subjective and objective values [5]. Same device was employed to measure the value of the vault, and it was discovered that in some circumstances the center vault increased in the case of myopia, because of the motion generated by connect with the crystalline [11]. In same year, Alfonso and his group followed up patients and measured the vault after a week, a month later, after 3 months, and yearly post-operative, they noticed that there was a significant decrease in the value of vault after the surgery, especially in the first six months. These statuses seen heavily in the eyes that have a very high vault [12].

Pentacam has used to determine the extent of change in the vault after a year of ICL implantation. The value of the vault began to change after one month of surgery.

The value of the vault decreased significantly, but after three months, the decrease was very low. Generally, the vault tends to decline after the operation [13]. In 2016, for measure the vault and anterior chamber (AC) angle width, following V4C ICL implantation, pentacam was employed for this purpose, and the result was the appearance of a relationship between the (AC) angle and the vault [14].

UBM is a technical tool used for imaging of the anterior segment of the eye, it had employed in 2011 to measure the vault and showed that in cases of low pIOL vaulting, a care should take specially with the cases which have vault value under 52 µm, and patient age is over 45 years, that these components increment the hazard for cataract [15]. The prediction of vault value after ICL implantation depends on many biometric factors preoperative, such as (horizontal sulcus-to-sulcus distance (STS) or WTW). The predictability of the vault will not accurate if it based solely on horizontal eye pressure. but the predict should be depends on another factors, such as compression by the iris, dampening effect of the ciliary sulcus structure, or innate ICL vault in order to avoid the incorrect prediction [16]. After all, a study in 2018 aimed at dividing clinical factors affecting the vault after surgery. Where the relationship between the vault value postoperative, and a number of factors such as ACD, WTW, and STS have examined. Where 236 eyes patients their vault values were between 250 µm and 750 µm has analyzed using different statistical methods. The results show that when the size of the pupil preoperative is large, greater preoperative ACD, and longer preoperative axial length, the vault will inevitably be high [17].

Ophthalmologists are trying to measure vault by using some devices to conduct their researches, where two types of lenses were implanted V3 or V4 for the study of cataract formation, and also for the study of the causes of the formation, where 75 eyes were followe up for three months. The results indicated that the formation of cataract increased during the follow-up period, especially older patients. Therefore, it has recommended making the value of vault higher than 0.15 mm to ensure that there is no friction between the ICL and crystalline lens [18].

In a specific study, the value of the vault was measured over a period of one month, three months, and one year. The focus was also on the change in the vault and its relation to refraction. The result appears that the vault is reduce over time, and the results revealed that the vault does not affected fraction and vice versa [19].

Alfonso and his team in their study, which also intended to measure the change in the value of the vault after surgery, revealed that the vault decreased after the third months of lens implantation. It is worth noting that the experiment has conducted on 964 eyes during 36 months [12].

MATERIALS AND METHODS

Pentacam

One of the tools that is used to get the data is called Pentacam, it is a rotation imaging technology, employed to measure the anterior and posterior corneal surface as well as segment structures, and produce number of images for corneal from different angles that give chance to select image with suitable angle to measure ICL vault precisely [1, 20].

pentacam obtain the image by rotating a charge coupled device camera (CCD) with synchronous pixel sampling as shown in Fig. 2, the system is consist of two camera, UV-free blue light; first camera is located in the center, and the second is positioned on rotation wheel which give capability to get a comprehensive image start from anterior surface of cornea ended to posterior surface the lens [21], which is the interested area for study.

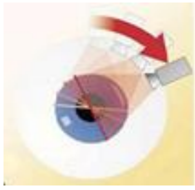

Fig. 2 Diagrammatic represent rotation camera

Feature extraction

Instead of using the value of pixels of the image where the image consist of two dimension array, it is more suitable if extract a set of number that are able to represent the characteristics of the image, this set of useful number is called vector and the method for extract the characteristic is known as feature extraction [22].

Edge histogram descriptor (EHD)

The chief function of this descriptor is illustrating the edges of an image, where image symbolizing five forms of the edge in each local area, partitioning image into parts called sub-image for each, where it alienated into 4x4 non-overlapping chunks as in Fig. 3.

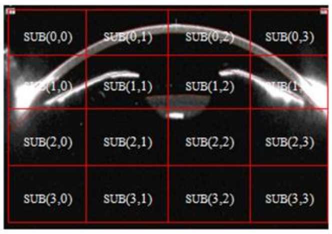

Fig. 3 Image divided into 16 pieces

Histogram of each sub-image has generated to gain the characteristics of the images, vertical, horizontal, 45-degree diagonal, 135-degree diagonal and non-directional edges, as shown in Fig. 4 where it is contained five bines each bin corresponding one form of the edge.

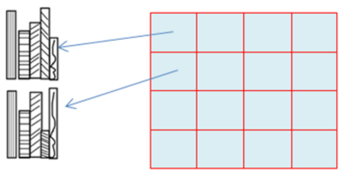

Fig. 4 Five types of edge bins for each sub-image.

A one-dimensional array of 80 bins was composed, by taking the histogram of all 16 blocks as illustrated in Fig. 5 started from sub-image (0, 0) to (3, 3) sub-image

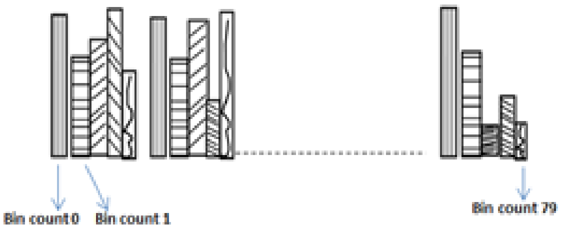

Fig. 5 A 1-D array of 80 bins of EHD

These 80 histogram bin is pass in two phases, first one is normalization this is, by divided the number frequency edge for each bin by total number of image–block in sub-image, Fig. 6 represent the image–block, which is the simple unit for get the edge, this unit is has specify whether it has edge or not and what is the predominate edge, the histogram value of the corresponding edge bin increases by one, Otherwise, the image-block without edge. The second phase is quantization, due to normalization the values are in small range; therefore, it should be decode bits for each edge type [23].

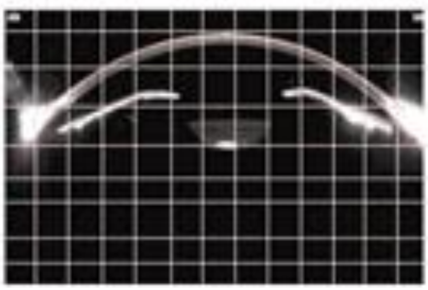

Fig. 6 Image-block.

Color layout descriptor (CLD)

Color feature is significant feature in images, which represents the color resolution-invariant and spatial distribution representation, so CLD is presume a good choice to extract this feature, that it is widely used in image processing applications [24].

Four steps should performed by this descriptor so that it can extract the characteristics of the image as shown in Fig. 7. Firstly, the image is partition into 8x8 sub-images, second step is dominant color selection for each block by use any method to dominant a single color, third step is handled the component (Y, Cb and Cr) of color image by discrete cosine transform (DCT) that is result three group of coefficients. Lastly, custom the zigzag scanning to extract the low frequency from the DCT coefficients, Which in turn produces color layout descriptor, Fig. 8 illustrate the block diagram of CLD extraction [25].

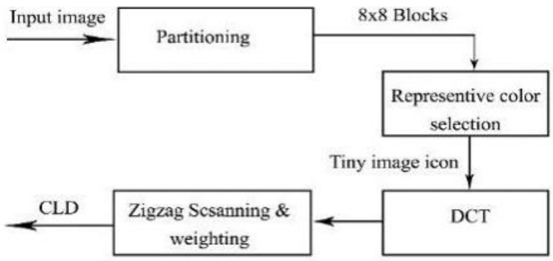

Fig. 7 The block diagram of the CLD extraction

Matching could be achieve by calculate the distance between two color layout descriptors through (1)

$$D = \sqrt{\sum_{k(Y)} w1_i (Y_1 - Y_1')^2} + \sqrt{\sum_{k(Cb)} w2_i (Cb_1 - Cb_1')^2} + \sqrt{\sum_{k(Cr)} w3_i (Cr_1 - Cr_1')^2} \quad (1)$$

The retrieval result obtained as a set of retrievals whose distance is less than a certain threshold d [26].

Naïve Bayes classifier

Recently, the Naive Bayes classifier become very popular due to it is simple since features are independent given class, and it performs surprisingly well [27, 28]. Feature is trained separately making it simple especially when it large number, because the independence of features. it is a try to make a specific instance belonging to a specific class, it is conducted by calculate the probability of how much this case strongly belonging to particular class, for a given class, naive Bayes assume that the feature is conditionally independent.

Given an example X, described by its feature vector $(x_1, \dots, x_n)$, we are looking for a class C that maximizes the likelihood that shown in (2).

$$P(X \mid C) = P(x_1, \dots, x_n \mid C) \quad (2)$$

Naïve Bayes assumption of conditional independence among the features, given the class, allows us to express this conditional probability $P(X \mid C)$ as a product of simpler probabilities [29] as illustrated in (3).

$$P(X \mid C) = \prod n_i = 1 P(x_i \mid C) P(X \mid C) = \prod_i = 1 n P(x_i \mid C) \quad (3)$$

Several factors that make Naïve Bayes not working properly, those factors summarized into three points, firstly, training data noise; which is appear when the method of training data be selected in non-proficient manner, which it could be reduced the training data noise by choosing appropriate method for data training. secondly, is bias, this type of error is happen when the data is crowded because it huge, and finally, factor is variance, which is appear when the data so small groups [30]. The unbalanced (different number of positive and negative example) data is a big defiance in training this classifier, that could causes a bad performance in its task [29].

Decision tree classifier (DT)

Decision tree classifier is one algorithm of the machine learning technique; it is very popular use as multistage table look-up rule [31]. According to the DT learning algorithm, the root is constructed, then it separate recursively till the end of the algorithm, consequently[32], a complete decision tree built as shown in Fig. 8.

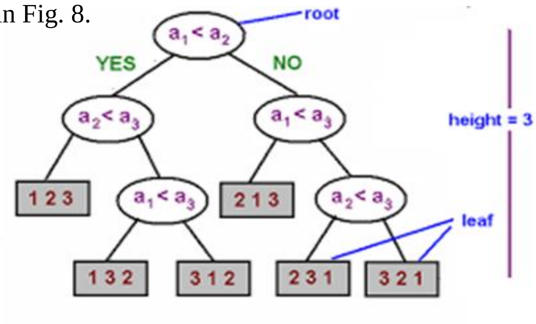

Fig. 8 Example of Decision Tree algorithm

Most significant feature in this classifier is that DT has capability to classify the unseen data, easy to user to update and training the data, finally, it has skill to simplify the structure, consequently, the classifier ready to select appropriate tree structure, and feature subsets should be used at each internal node [33]. To design the structure of tree DT could select minimum error rate, min-max path length, minimum number of nodes in the tree, minimum expected path length, or maximum average mutual information gain etc. [34].

C4.5 is one of the DT algorithms; it is popular for classification purpose [35]. Initiated by calculates the information of properties at each node, then choose the highest information gain ratio that evaluated using entropy law [36]. For instance D is a dataset and that A_i is one of the dataset. And there are a set of classes, $C_1, C_2, \dots \dots, C_m$. Then information gain is as (4) and (5).

$$\mathrm{Gain}(D, A_i) = \mathrm{Entropy}(D) - \sum_{i \in \mathrm{Value}(A_i)} \frac{|D_i|}{D} \mathrm{Entropy}(D_i) \quad (4)$$

Where

$$\mathrm{Entropy}(D) = -\sum_{i=1}^{m} \frac{\mathrm{freq}(C_i, D)}{|D|} \log_2 \frac{\mathrm{freq}(C_i, D)}{|D|} \quad (5)$$

Where $\mathrm{freq}(C_i, D)$ represent examples numbers in the dataset D belong to class C_i and D_i divided by attribute A_i value. Then $\mathrm{SplitInfo}(A_i)$ is define as the information content of the attribute A_i itself as illustrated in (6) and (7).

$$\mathrm{SplitInfo}(D, A_i) = -\sum_{i \in \mathrm{Value}(A_i)} \frac{|D_i|}{D} \log_2 \frac{|D_i|}{D} \quad (6)$$

The gain ratio is the information gain calibrated by splitInfo:

$$\mathrm{Gain\ Ratio}(D, A_i) = \frac{\mathrm{Gain}(D, A_i)}{\mathrm{SplitInfo}(A_i)} \quad (7)$$

METHODS

In order to discover a new information about a specific subject or understanding it better, it should be there a particular way to studying by set of specific techniques for selecting cases, measuring and observing aspects, gathering and refining data, and analysing data then reporting on result [37], Accordingly, in order to satisfy the objectives of this work, a quantitative research was held, which involves data in the form of numbers and statistics [38], and use precise measurement to predict hypotheses.

first of all the dataset partitioning into two specific parts, normal vaults and non-normal vaults, the normal set are images that content the segment of cornea with suitable vault, whereas the non-normal set are images of segment of cornea with unsuitable vault. Then a complete system has been built, which is consist of two main phases, the first phase is features extraction where the features has extracted from the input dataset for training the system, second phase is classification, where one classifier has been used to conduct the classification process, that predict to which class the test image belong[37].

There are several algorithms has been built to achieve the aim of the system, in first experiment, Edge histogram descriptor has employed to extract the characteristics of training dataset, vectors of features was generated, that stored in excel file to be used as an aspect tool for matching and retrieve the content of the test image. After composed the feature vector, the classifier could be used as a tool for classify the test image, in the experiment Naïve Bayes has been used, which is it has ability to classifying content of images easily [39].

In second experiment, EHD had used again for extract the characteristics of training dataset, decision tree classifier is employed for classification phase, after all, the decision has made about content of the test image either normal or non-normal vault.

Third experiment, CLD descriptor is used here for extract the features of the training dataset, that generate vectors which appear the color resolution-invariant and spatial distribution representation, Naïve Bayes classifier is use to classify the test image by using the vectors that have generated from CLD descriptor. Finally, DT classifier has been employed for classify the test image through using the vectors of features that are produced from CLD descriptor that has saved in excel file.

RESULT AND DISCUSSION

A. Results

The accuracy and efficiency of the proposed algorithms estimated through the proposed system on datasets and calculate the accuracy using (8).

$$Precision_{(i)} = \frac{\text{Correctly defects detected}_{(i)}}{\text{Total images tested containing defect}_{(i)}} * 100 \quad (8)$$

Consequently, apply the proposed algorithms, on dataset that represent an images included the background and the cornea with vault. The results that obtained from analyzing the objects in these images were it used to detect the content of the image under investigation. Table I shows the result of applying the proposed algorithms on datasets that are representing the accuracy that has calculated using equation 8.

TABLE I. THE ACCURACY PERCENTAGE (%)

Classifier / Descriptor	EHD	CLD
Naïve Bayes	65	95.5
Decision Tree	54.6	66.6

It is obvious from the data in the table above that these algorithms is very applicable for prescribe and identification for any input images of the system, below table II illustrate the time required for applyıng each algorithm on test image.

TABLE II. THE EXECUTION TIME (SECONDS)

Execution tıme / Descriptor	EHD	CLD
Naïve Bayes	0.025	0.23
Decision Tree	0.34	0.54

B. Discussion

In terms of accuracy, the analysis of data presented in Tables 1 indicate that applying of Naïve Bayes were better than those of Decision Tree. Naïve Bayes appears better because the features of each test image compared with all the features of the trained image in Naïve Bayes method, whereas same feature compared with less than a half of trained features in DT classifier because of the way this algorithm works. Therefore, the precision of Naïve Bayes annotation was higher.

On the other hand, content of the images, that its features were extracted with EHD algorithm, were retrieval wrongly, because of the similarity of the image content in both partitions the normal and non-normal vault, where the differences is unpretentious that classifier cannot recognized them easily.

CLD uses the colors within images, therefore, observed that by using this descriptor with Naive Bayes classifier give result more accurately than using it with DT classifier. CLD with Naive Bayes classifier enable the system to recognize the normal vault images from the another, that make it gives satisfy efficient results, but it cannot reach 100% accuracy because in some images from different classes, have a similarity of subject colors that produce weakness in system performance.

In term of time, executing time of the system, for test images, that employed the Naïve Bayes classifier in general was better in comparison with DT classifier, because the calculation process of information gain in C4.5 algorithm involved the compute of log function, and the time consuming of the log function is causes a problem on total computation time.

VI. Conclusion

Retrieve the content of the image successfully is depend on many factors, such as, how to extract the characteristic of the image efficiently, how to select the suitable descriptor which is built on the basis of the nature of the image content, the classifier capability for dealing with the descriptors outputs in order to conduct the classification process, and overcome the challenge that is caused by the difference between the concept of high level and low level feature of the image. In this work, a smart algorithm presented mainly for texture and color based features that are the strengths to improve the precision of system, reduce the system execution time, growth the system efficiency, and increase data training velocity.

REFERENCES

[1] Lackner, B., Pieh, S., Schmidinger, G., Simader, C., Franz, C., Dejaco-Ruhswurm, I., & Skorpik, C. (2004). Long-term results of implantation of phakic posterior chamber intraocular lenses. *Journal of Cataract & Refractive Surgery*, *30*(11), 2269-2276.

[2] Pineda-Fernández, A., Jaramillo, J., Vargas, J., Jaramillo, M., Jaramillo, J., & Galíndez, A. (2004). Phakic posterior chamber intraocular lens for high myopia. *Journal of Cataract & Refractive Surgery*, *30*(11), 2277-2283.

[3] Chen, X., Miao, H., Naidu, R. K., Wang, X., & Zhou, X. (2016). Comparison of early changes in and factors affecting vault following posterior chamber phakic implantable collamer lens implantation without and with a central hole (ICL V4 and ICL V4c). *BMC ophthalmology*, *16*(1), 161.

[4] Lee, H., Kang, S. Y., Seo, K. Y., Chung, B., Choi, J. Y., & Kim, K. S. (2014). Dynamic vaulting changes in V4c versus V4 posterior chamber phakic lenses under differing lighting conditions. *American journal of ophthalmology*, *158*(6), 1199-1204.

[5] Alfonso, J. F., Lisa, C., Palacios, A., Fernandes, P., González-Méijome, J. M., & Montés-Micó, R. (2009). Objective vs. subjective vault measurement after myopic implantable col-

lamer lens implantation. *American journal of ophthalmology*, *147*(6), 978-983.

[6] Zaldivar, R. O. B. E. R. T. O., Oscherow, S. U. S. A. N. A., & Piezzi, V. (2003). Bioptics: Our personal experience. *LASIK: Advances, Controversies and Customs. Slack Inc., Thorofare New Jersey*, 249-257.

[7] Elies, D., Coret, A., Puig, J., & Rombouts, A. (2004). Protocolo en el implante de lentes fáquicas tipo ICL. *Annals d'oftalmologia*, *12*(1), 30-34.

[8] Bechmann, M., Ullrich, S., Thiel, M. J., Kenyon, K. R., & Ludwig, K. (2002). Imaging of posterior chamber phakic intraocular lens by optical coherence tomography. *Journal of Cataract & Refractive Surgery*, *28*(2), 360-363.

[9] Koivula, A., & Kugelberg, M. (2007). Optical coherence tomography of the anterior segment in eyes with phakic refractive lenses. *Ophthalmology*, *114*(11), 2031-2037.

[10] Schmidinger, G., Lackner, B., Pieh, S., & Skorpik, C. (2009). Long-term changes in posterior chamber phakic intraocular collamer lens vaulting in myopic patients. Ophthalmology,117(8), 1506-1511.

[11] Lindland, A., Heger, H., Kugelberg, M., & Zetterström, C. (2012). Changes in vaulting of myopic and toric implantable Collamer lenses in different lighting conditions. *Acta ophthalmologica*, *90*(8), 788-791.

[12] Alfonso, J. F., Lisa, C., Abdelhamid, A., Fernandes, P., Jorge, J., & Montés-Micó, R. (2010). Three-year follow-up of subjective vault following myopic implantable Collamer lens implantation. *Graefe's Archive for Clinical and Experimental Ophthalmology*, *248*(12), 1827-1835.

[13] Du, G. P., Huang, Y. F., Wang, L. Q., Wang, D. J., Guo, H. L., Yu, J. F., ... & Huang, H. B. (2012). Changes in objective vault and effect on vision outcomes after implantable Collamer lens implantation: 1-year follow-up. *European journal of ophthalmology*, *22*(2), 153-160.

[14] Eissa, S. A., Sadek, S. H., & El-Deeb, M. W. (2016). Anterior chamber angle evaluation following phakic posterior chamber Collamer lens with CentraFLOW and its correlation with ICL vault and intraocular pressure. *Journal of Ophthalmology*, *2016*.

[15] Maeng, H. S., Chung, T. Y., Lee, D. H., & Chung, E. S. (2011). Risk factor evaluation for cataract development in patients with low vaulting after phakic intraocular lens implantation. *Journal of Cataract & Refractive Surgery*, *37*(5), 881-885.

[16] Lee, D. H., Choi, S. H., Chung, E. S., & Chung, T. Y. (2012). Correlation between preoperative biometry and posterior chamber phakic Visian Implantable Collamer Lens vaulting.*Ophthalmology*, *119*(2), 272-277.

[17] Lee, H., Kang, D. S. Y., Choi, J. Y., Ha, B. J., Kim, E. K., & Seo, K. Y. (2018). Analysis of pre-operative factors affecting the range of optimal vaulting after implantation of 12.6-mm V4c implantable Collamer lens in myopic eyes. *BMC Ophthalmology*, *18*(1), 163.

[18] Gonvers, M., Bornet, C., & Othenin-Girard, P. (2003). Implantable contact lens for moderate to high myopia: relationship of vaulting to cataract formation. *Journal of Cataract & Refractive Surgery*, *29*(5), 918-924.

[19] Kamiya, K., Shimizu, K., & Kawamorita, T. (2009). Changes in vaulting and the effect on refraction after phakic posterior chamber intraocular lens implantation. *Journal of Cataract & Refractive Surgery*, *35*(9), 1582-1586.

[20] Barkana, Y., Gerber, Y., Elbaz, U., Schwartz, S., Ken-Dror, G., Avni, I., & Zadok, D. (2005). Central corneal thickness measurement with the Pentacam Scheimpflug system, optical low-coherence reflectometry pachymeter, and ultrasound pachymetry. *Journal of Cataract & Refractive Surgery*, *31*(9), 1729-1735.

[21] Jain, R., & Grewal, S. P. S. (2009). Pentacam: principle and clinical applications. *Journal of Current Glaucoma Practice*, *3*(2), 20-32.

[22] Li, X., Chen, S. C., Shyu, M. L., & Furht, B. (2002). Image retrieval by color, texture, and spatial information. *8th Inter. Con. on Dis. Multi. Sys.(DMS'2002), San Francisco Bay, California, USA*, 1-8.

[23] Frigui, H., and Gader, P. (2009). Detection and discrimination of land mines in ground-penetrating radar based on edge histogram descriptors and a possibilistic $ k $-nearest neighbor classifier. *IEEE Transactions on Fuzzy Systems*, *17*(1), 185-199.

[24] Kasutani, E., & Yamada, A. (2001). The MPEG-7 color layout descriptor: a compact image feature description for high-speed image/video segment retrieval. In *Image Processing, 2001. Proceedings. 2001 International Conference on* (Vol. 1, pp. 674-677). IEEE.

[25] Manjunath, B. S., Ohm, J. R., Vasudevan, V. V., & Yamada, A. (2001). Color and texture descriptors. *IEEE Transactions on circuits and systems for video technology*, *11*(6), 703-715.

[26] Manjunath, B. S., Salembier, P., & Sikora, T. (Eds.). (2002).*Introduction to MPEG-7: multimedia content description interface* (Vol. 1). John Wiley & Sons.

[27] Friedman, N., Geiger, D., & Goldszmidt, M. (1997). Bayesian network classifiers. *Machine learning*, *29*(2-3), 131-163.

[28] Rish, I. (2001, August). An empirical study of the naive Bayes classifier. In *IJCAI 2001 workshop on empirical methods in artificial intelligence* (Vol. 3, No. 22, pp. 41-46). New York: IBM.

[29] Yousef, M., Nebozhyn, M., Shatkay, H., Kanterakis, S., Showe, L. C., & Showe, M. K. (2006). Combining multi-species genomic data for microRNA identification using a Naive Bayes classifier. *Bioinformatics*, *22*(11), 1325-1334.

[30] Mukherjee, S., & Sharma, N. (2012). Intrusion detection using naive Bayes classifier with feature reduction. *Procedia Technology*, *4*, 119-128.

[31] Haralick, R. M. (1976). The table look-up rule. *Communications in Statistics-Theory and Methods*, *5*(12), 1163-1191.

[32] Perner, P. (Ed.). (2014). *Machine Learning and Data Mining in Pattern Recognition: 10th International Conference, MLDM 2014, St. Petersburg, Russia, July 21-24, 2014, Proceedings*(Vol. 8556). Springer.

[33] Kurzyński, M. W. (1983). The optimal strategy of a tree classifier. *Pattern Recognition*, *16*(1), 81-87.

[34] Quinlan, J. R., & Rivest, R. L. (1989). Inferring decision trees using the minimum description lenght principle. *Information and computation*, *80*(3), 227-248.

[35] Li, Y., Yang, Q., Lai, S., & Li, B. (2015, January). A new speculative execution algorithm based on C4. 5 decision tree for Hadoop. In *International Conference of Young Computer Scientists, Engineers and Educators* (pp. 284-291). Springer, Berlin, Heidelberg.

[36] Safavian, S. R., & Landgrebe, D. (1991). A survey of decision tree classifier methodology. *IEEE transactions on systems, man, and cybernetics*, *21*(3), 660-674.

[37] Johnson, R. B., & Onwuegbuzie, A. J. (2004). Mixed methods research: A research paradigm whose time has come.*Educational researcher*, *33*(7), 14-26.

[38] Taylor, S. J., Bogdan, R., & DeVault, M. (2015). Introduction to qualitative research methods: A guidebook and resource. John Wiley & Sons.

[39] Lewis, D. D. (1998, April). Naive (Bayes) at forty: The independence assumption in information retrieval. In *European conference on machine learning* (pp. 4-15). Springer, Berlin, Heidelberg.

CURRICULUM VITAE

Name and Surname : Hala Zaid ABDULHAMEED

Address : Baghdad, Iraq

E-mail address : **hala_85h@yahoo.com**

EDUCATION INFORMATION

Undergraduate : Baghdad University, 2003-2007

Master : Aksaray University, 2019

PUBLICATIONS, PRESENTATIONS AND PATENTS

1. Hala Zaid ABDULHAMEED and Dr. Nebras Hussein,"A Smart Algorithm to Predict the Post-operative Parameters of Intra – corneal Lens", International Journal of Computer Science and Information Security, Paper ID 31121813, Vol. 17 No. 1 JAN 2019**.**